University of Nevada, Reno

Network Behavior in Thin Film Growth Dynamics

A dissertation submitted in partial fulfillment of the requirements for the degree of

Doctor of Philosophy in Computer Science and Engineering

By

Satish K. Badepalli

Dr. Murat Yuksel / Dissertation Advisor

May 2017

THE GRADUATE SCHOOL

We recommend that the dissertation
prepared under our supervision by

SATISH K. BADEPALLI

Entitled

Network Behavior in Thin Film Growth Dynamics

be accepted in partial fulfillment of the
requirements for the degree of

DOCTOR OF PHILOSOPHY

Dr. Murat Yuksel, Ph.D., Advisor

Dr. George Bebis, Ph.D., Committee Member

Dr. Sergiu Dascalu, Ph.D., Committee Member

Dr. Mehmet Gunes, Ph.D., Committee Member

Dr. Dhanesh Chandra, Ph.D., Graduate School Representative

David W. Zeh, Ph. D., Dean, Graduate School

May, 2017

Abstract

Understanding patterns and components in thin film growth is crucial for many engineering applications. Further, the growth dynamics (e.g., shadowing and re-emission effects) of thin films exist in several other natural and man-made phenomena. Recent work developed network science techniques to study the growth dynamics of thin films and nanostructures. These efforts used a grid network model (i.e. viewing of each point on the thin film as an intersection point of a grid) via Monte Carlo simulation methods to study the shadowing and re-emission effects in the growth. These effects are crucial in understanding the relationships between growth dynamics and the resulting structural properties of the film to be grown. In this dissertation, we use a cluster-based network model with Monte Carlo simulation method to study these effects in thin film growth. We use image processing to identify clusters of points on the film and establish a network model of these clusters. Monte Carlo simulations are used to grow films and dynamically track the trajectories of re-emitted particles. We treat the points on the film substrate and cluster formations from the deposition of adatoms / particles on the surface of the substrate as the nodes of network, and movement of particles between these points or clusters as the traffic of the network. Then, graph theory is used to study various network statistics and characteristics that would explain various important phenomena in the thin film growth. We compare the cluster-based results with the grid-based results to determine which method is better suited to study the underlying characteristics of the thin film. Based on the clusters and the points on the substrate, we also develop a network traffic model to study the characteristics and phenomena like fractal behavior in the count and inter-arrival time of the particles. Our

results show that the network theory of the growth process explains some of the underlying phenomena in film growth better than the existing theoretical and statistical models.

Table of Contents

Chapter 1 Introduction

Network science is an emerging and highly interdisciplinary field that aims to develop theoretical and practical techniques to study natural and man-made networks. It studies various concepts of networks that exist in diverse fields such as biology, physics, technology and social relations. It compares, contrasts and integrates techniques, algorithms, and models developed in fields like mathematics, computer science, statistics, and physics [1]. The network science plays a crucial role in understanding various phenomena occurring in natural, biological, social models. Technological advances in the last few decades have given unprecedented increase in available data. Many of the complex phenomena occurring in these diverse fields have been successfully explained using networks [2]. Increasing amounts of data is being captured and is actively being studied in networks, like food webs and structure of human social networks [3-6], are becoming available. Various scientists use this large data to study universal laws of physics. The results of these studies have raised much interest in network science. Many networks that occur in nature have shown to share global statistical features of "small world networks" [7], which is a common pattern in data communication networks. For example, unexpected similarities are observed between social networks and the Internet [8-10].

Network science deals with wide variety of concepts like graph theory, statistical methods, data mining, and predictive analysis. Historically, networks are studied as part of graph theory. Sociologists are one of the earlier groups to study networks for explaining various sociological relations. These studies usually include distribution of questionnaires, and asking respondents to detail their interactions with others and seeking a networking behavior among various participant groups [11]. The study of networks came a long way

since these early studies. Current challenges for network science are understanding and characterizing highly *complex* and *dynamic* behaviors exhibited in the networks at hand, particularly in nature. Current network science research focus is on statistical analysis of *large* number of nodes and edges. This focus is largely aided by the advent of computers and communication network that can collect and analyze data at large scales [12]. In traditional network engineering, the systems and prototypes are modeled based on the desired or envisioned output. In network science, the models and prototypes are based on the input. The network is modeled based on deep analyses of available facts and existing features of various components of the system. Current research is not only focused on applying existing theories and models to real data or situations, but also on studying dynamic processes of these complex networks [13].

In the last decade, the network science has gained enormous popularity among other disciplines. One of the main reasons behind this is the discovery that, despite apparent differences, fundamental laws and reproducible mechanisms are driving the evolution of networks. The increased interest in study of network science can also be attributed to emergence of network map tools capable of revealing universality of network characteristics [14]. Even though many networks around us differ in size, nature, and complexity, they are more similar once we disregard the nature of components and their interactions. Comparing natural and man-made systems with networks have shed light into previously unknown phenomena in these systems. This paved the way to modeling many networks and their growth. Networks are studied for various properties like heavy-tailed degree distributions, heavy-tailed Eigenvalues, heavy-tailed Eigenvectors, small diameters, and shrinking or stabilizing diameters [97]. Network modeling can be divided into *mechanistic* [16, 17] and *statistical* models [18]. Copying model [17], community

guided attachment [16] and the forest fire model [16] belong to the former category. Erdös-R´enyi-Gilbert Random Graph Model, Exchangeable Graph Model and P1 Model belong to the latter group [130]. Static models deal with characterization of networks at a single snapshot of the network. Mechanistic models seek to model multiple snapshots of evolving networks [19].

The basic properties of graphs can be used to model a network and study its characters. Essentially a network can be represented as a graph with nodes of networks as vertex of graph and links between nodes as edges of the graph. In a social network, which intends to study the interaction between people, the nodes are the people and interactions between these people are links between the nodes. Similarly, in an actor network, which studies the casting relation between various actors, the actors are the nodes and a link is formed between two actors if they acted in same movie. One can observe that different elements and interactions between these elements can be represented as a similar or even the same network. In the following figure, even though the properties of nodes and their interactions are defined differently, the final network is same. Figure 1 (a) shows the network of three actors and their casting relation with each other.

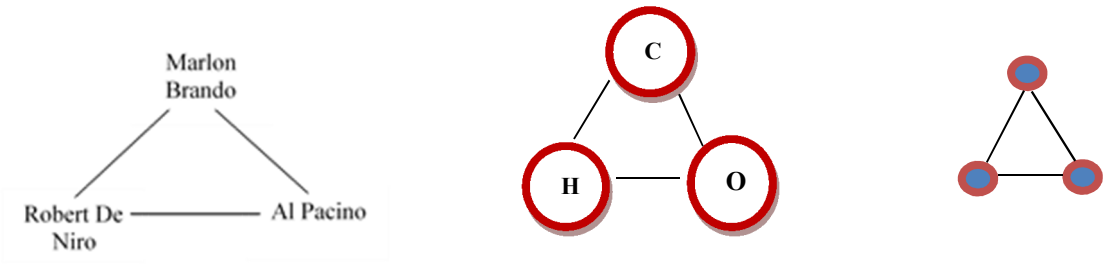

(a) *Hollywood Actor Network* *(b) Chemical Network* *(c) Generalized Graph*

***Figure 1**: Examples of real-world networks*

The actors are the nodes and a link is formed if they acted in the same movie. Figure 1 (b) shows relation between chemical reactants. The reactants are the nodes and the link is defined if they can form a chemical compound. The Figure 1 (c) is a generalized graph representation of the actor network and chemical network represented in Figure 1 (a) and 1 (b). This makes it easy to study the characteristics and calculate various measures by using network theory and models. The analysis of topology of these networks shed light on many underlying information. These networks not only help in studying a static system but also helps study informative measurements and connectivity of evolving systems over a period. This generality and ease of transforming various systems in to graphs propelled the interest from wide variety of fields to look in to network science for answers.

In this dissertation, we study the networking behavior in thin film growth. In our experiments, *the points on the substrate and clusters* formed on substrate are considered as *nodes* and *path of the ad-atoms* are mapped as *links* between these nodes. Movement of the ad-atoms between various points and clusters on the film are tracked and studied to determine the topology of network formed thus. This is discussed in detail in future chapters.

1.1 Network of Thin Film Growth

The demand for advanced materials with desirable properties by various industries has driven the development of thin film technology [20]. Since then, thin film development has become a major research area. Some of the application areas of thin film include microelectronics, optoelectronics, detectors, sensors, micro-electro-mechanical systems (MEMS), and more recently nano-electro-mechanical systems (NEMS) [21]. These

coatings have thickness ranging between nano- or micro- scales and are grown using vacuum deposition techniques [22-24]. Surface morphology of these thin film surfaces determines various physical and chemical properties. This makes it important to control and study the dynamics of the growth on the substrate so that the surface morphology and formations can be predicted prior to the growth. Commonly employed deposition techniques are thermal evaporation, sputter deposition, chemical vapor deposition (CVD), and oblique angle deposition. Different than others, oblique angle deposition technique [25-32] is typically used for the growth of nanostructured arrays of rods and springs through a physical self-assembly process. Kinetic Monte-Carlo (KMC) simulation provides a framework for modeling the effect of macroscopic process variables on the thin film microstructure and has been widely used to simulate CVD processes [20].

Flat thin films are desired for many applications. Thin film growth is a complex phenomenon that occurs away from equilibrium. Most of the deposition techniques create some form of surface roughness. Atoms are deposited unevenly at different times across the surface. This random arrival, which is part of the process creates the roughness on the substrate. The surface morphology of the thin film affects many physical and chemical properties. Hence it is of great interest to control and understand the surface morphology in thin film growth process [21].

In thin film growth simulations, the impact point on the lattice is randomly chosen to reflect the real growth process. However, particles that approach the surface at an angle can preferentially land on higher surface points before reaching the target point, which is called the *shadowing effect*. The particles can stick to the surface with a probability defined as the *sticking coefficient*. Particles that do not stick are re-emitted and can travel to another

surface point before settling down at a point on the lattice. These particles later take form into various clusters representing the hills and valleys of the rough surface. After the incident particle is deposited onto the surface, it becomes a so called “adatom”.

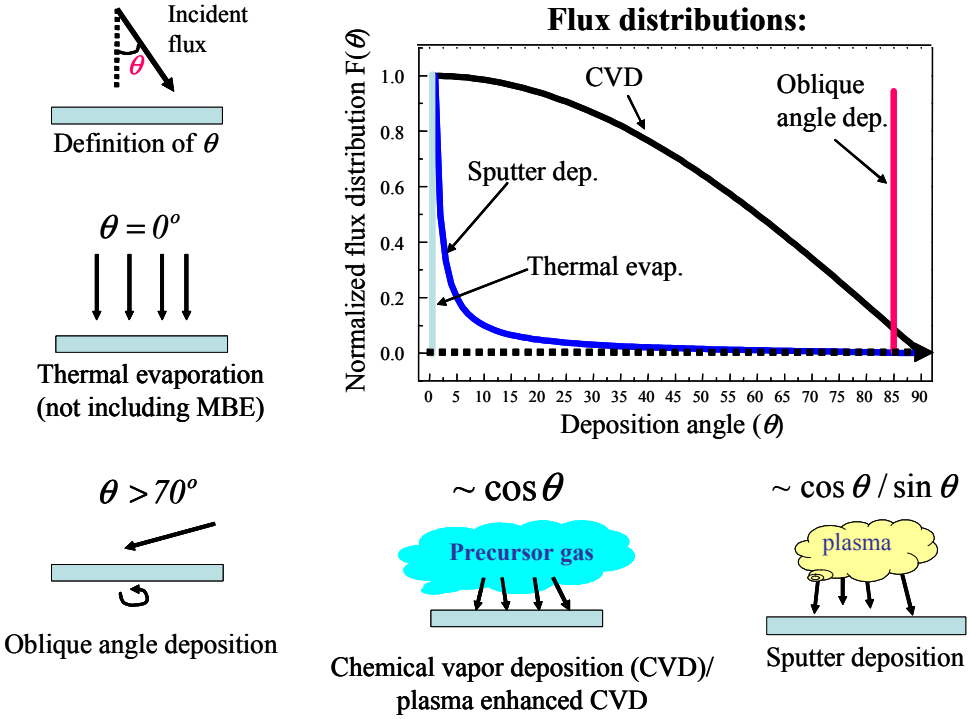

***Figure 2**: Commonly used thin film deposition techniques. [21]*

Figure 2 shows commonly employed deposition techniques: thermal evaporation, sputter deposition, chemical vapor deposition (CVD), and oblique angle deposition. Different than others, oblique angle deposition technique [25-32] is typically used for the growth of nanostructure arrays of rods and springs through a physical self-assembly process. Here we do not include the molecular beam epitaxy (MBE) technique that involves detailed interactions between the newly deposited adatoms and the surface steps [34]. These detailed interactions can generate a separate class of morphologies. The plot in Figure 2 also shows the incident flux distribution for various deposition techniques. The ‘θ’ is

defined as the angle between the surface normal and the direction of the incidence beam of atoms.

The atoms that are deposited on the lattice surface and the path they take during this course can be well depicted using graph theory. A graph is a set of vertices connected via edges. The vertices are also referred to as nodes in some cases [33]. In the diffusion methodology, the vertices or nodes of a graph can represent a single atom or a group of atoms that are related by a property like distance. The interaction between these atoms can be represented as edges between the nodes. The edges can be directional or non-directional. This theory forms the basis of our experiments. We use various properties of these atoms to form the topology of the network. Using this topology, we intend to study various properties of thin film growth.

1.2 Motivation and Significance

Conventional statistical methods cannot be used to describe the complex phenomenon of surface morphology formation in thin film growth due to its intractability. There have been numerous modeling and experimental approaches [34, 35] proposed based on dynamic scaling analysis. Experimental results and predictions of growth models have varied considerably [21].

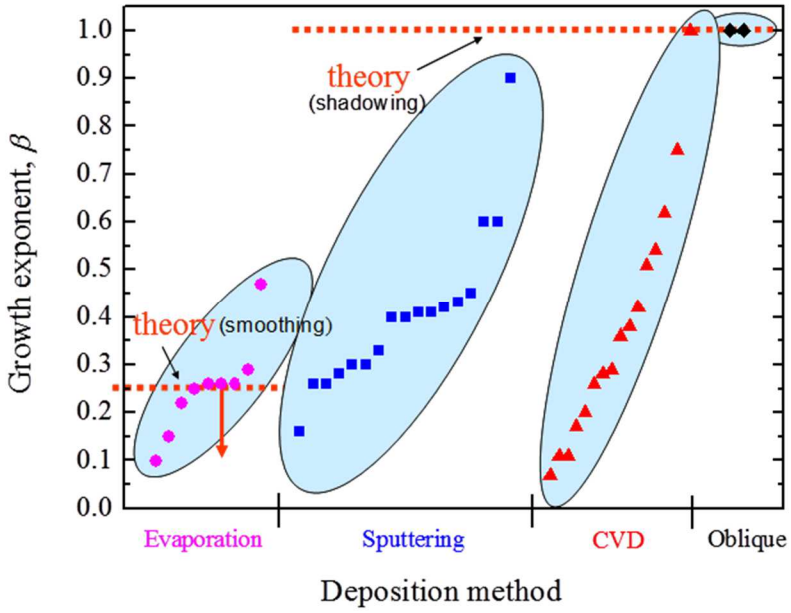

***Figure 3**: A survey of experimentally obtained values of growth exponent reported in the literature for different deposition techniques is compared to the predictions of common thin film growth models in dynamic scaling theory. Root-mean-square roughness (RMS) grows as a function of time in a power law form, where β is the "growth exponent" ranging between 0 and 1. β = 0 for a smooth growth front and β = 1 for a very rough growth front. [21]*

In Figure 3, a collection of experimental β values reported in the literature [36] is shown and these values are compared to the predictions of growth models. It can be clearly seen in Figure 3 that experimentally reported values of growth exponent β are far from agreement with the predictions of these growth models. Especially, sputtering and CVD techniques are observed to produce morphologies ranging from very small to very large β values indicating a "non-universal" behavior.

To better explain the surface growth dynamics, one should take into account the effects of both "shadowing" and "re-emission" processes [37-41]. During growth, particles approaching at oblique angles settle on higher surface points (hills) due to the shadowing effect. This results in formation of rougher surfaces with columnar structures that can also be engineered to form "nanostructures" under extreme shadowing conditions, as in the case

of oblique angle deposition that can produce arrays of nanorods and nanosprings [26-31]. Based on sticking coefficient of the material, the particles can stick or bounce of at their impact point. *Sticking coefficient is the overall likelihood of an atom/molecule sticking to the surface after complicated physical and chemical processes, and therefore represents a statistical average property of the incident flux interaction with the growing surface.* Non-sticking particles are re-emitted and can arrive at other surface points including shadowed valleys. In other words, re-emission has a smoothening effect while shadowing tries to roughen the surface. Both the shadowing and re-emission effects have been proven to be dominant over the surface diffusion and noise, and act as the main drivers of the dynamical surface growth front [29, 30]. The growth of a given surface point depends on the heights of near and far-away surface locations due to shadowing and existence of re-emitted particles that can travel over long distances. Only recently, it has been proposed that shadowing and re-emission effects could be fully incorporated into the Monte Carlo lattice simulation approaches [37-42, 44-47]. These simulations successfully predicted the experimental results on surface morphology including the β values shown in Figure 3. At small sticking coefficients (e.g., $s < 0.5$) re-emission was stronger than the roughening effects of shadowing and Monte Carlo simulations produced smooth surfaces with small β values. At higher sticking coefficient values, shadowing effect becomes the dominant process and columnar rough morphologies start to form. These Monte Carlo simulations also successively reproduced the morphologies and exponents predicted by the well-known Kardar-Parisi-Zhang (KPZ) [48] model in dynamic scaling theory, for the case where small sticking coefficient particles were re-emitted multiple times and resulted in a conformal growth [45]. Like experiments, it was not possible to capture a “universal” growth behavior using Monte Carlo simulation.

Conventional growth models fail to explain most of the experimental results for dynamic growth and dynamic scaling breaks down when shadowing is present. Since most of the commonly used deposition techniques has shadowing affect, dynamic scaling cannot be used in such cases. On the flip side, universal behavior in growth processes cannot be explained using simulation techniques. On top of it the simulations that can explain the experimental results are hard to implement by researchers. This emphasizes the need of more robust and easy-to-implement modeling techniques for capturing analytical and empirical relations in dynamic thin film growth [21].

Further, using network modeling and science to capture growth patterns is applicable to areas other than thin films as well. With similar local mapping of growth dynamics to a network, various social and physical phenomena can be modeled as a network; and hence, be analyzed using network science techniques. For example, wealth growth in a society may be modeled as a network if a business transaction is considered as a "link" while individuals or institutions are considered as "nodes" [131]. Similar to what we propose about explaining the thin film surface morphology via network properties, properties of wealth growth and its distribution could potentially be explained via the characteristics of the corresponding network.

In past decade, various physical, chemical, biological phenomena have been explained using network concepts [2, 33, 51, 52]. Various aspects and features of these phenomena are mapped to network topology and characteristics and are studied from a network perspective. These studies help us to better understand underlying behavior and interaction between various components. For example, a protein network help scientists to study the interaction between various proteins. It is observed that these interactions form a highly-

connected network. These interactions help scientists find more comprehensive understanding of protein function and cellular interactions [53].

This dissertation is built on top of earlier work by Karabacak and Yuksel et al. [21, 54] to map the thin film growth to a network model, and apply network modeling concepts to study the particle movement and surface growth phenomena. In the early work, each point of a substrate is treated as a node of network and the movements of ad-atoms are mapped as edges of the network. Then, the degree and distance distributions of this network are studied in this work.

In this dissertation, we aim to further this work so that it can better capture the growth dynamics and patterns. We, for example, enhance the topology of the network of thin film growth by treating *clusters* forming on the film surface as different nodes and establish a different "cluster-based" network model of the growth. Our initial results show that the shadowing effect during the film growth is better captured by the cluster-based network model [129] in comparison to the cluster-based network model in [54]. Further, on top of these cluster-based or cluster-based network models, we intend to establish a traffic model of the growth process to study various traffic characteristics of these two networks and compare them to other real-world network traffic. We believe by doing this we would better understand the behavior of ad-atoms movement on the surface of a thin film substrate. We would also be able to better understand the shadowing and smoothing effects of the thin film. This understanding could be used to better engineer the thin film growth.

1.3 Contributions

In this dissertation, we proposed a cluster-based model to study important characteristics of thin film growth like shadowing affect and smoothing affect. We compared this method with earlier proposed grid-based network model. The grid-based model is effective to study the local interactions between the particles and how these interactions affect the growth of the thin film and formation of hills and valleys. Our proposed cluster-based model studies global behaviors of particles that are similar in nature. By doing this the focus of the study shifts to actual hills and valleys which influence the thin film growth phenomenally compared to individual points on the substrate. We also developed a traffic model using the movement of the particles to study the properties of the particle movement that happen during the thin film growth. Using this model, we studied the inter-arrival times of the particles and identified various patterns in particles using the existing network traffic models. These studies give us new network modeling based insights on how various factors like sticking coefficient of the material and thickness of the film would impact the growth. Some of the key findings our work are as follows:

- The sticking coefficients and the film thickness have dominant effect on the formation of the clusters. At lower sticking coefficients and lower thickness of the film, distinct clusters are not formed. At higher sticking coefficients, distinct clusters are formed as the thickness of the film grows.
- Our clustering approach significantly simplifies understanding the stochastic shadowing and re-emission effects by not recording the properties and behavior of the particles that are similar because of their physical position on the film.
- With the cluster-based model, the degree distribution of the network model of the growth process seems to move more towards power law, indicating that some of

the clusters have significantly more links (particle emissions) than the others and act as hubs of particle re-emissions. This reveals that the columnar structures (i.e., the clusters in our model) are more inter-dependent and the emergence of a columnar structure requires existence of these hubs during the film growth process.

- The power exponent of the network does not change when the factors like sticking coefficient, angle of incidence and thickness of film are changed in the cluster-based model. This demonstrates a universal behavior in the thin film growth network.
- The density of the cluster-based network is very low. This suggests that majority of adatom particle movements are local. Further, the results show that smoothing effect is not prominent between clusters.
- With the cluster-based network, we can also observe that diameter and average path length of the network are larger, which suggests that particle movements between clusters has decreased – a property of the shadowing effect.
- The above observations show the cluster-based model is better suited to study global behaviors of thin film growth and particularly the shadowing phenomenon.
- The Hurst parameter of the particle traffic on the cluster-based network is 0.76, which shows a long-range dependency similar to the Internet traffic and quantifies the fractal behavior of the particle movements.

Chapter 2 Literature Review

2.1 Thin Films

Most materials used in high technology applications are composites. They have different properties at the surface when compared to the core. This is extremely desirable when one needs to have a material to exhibit various properties that cannot be found in a single material. The combination of materials will give the desired results. An example of industrial requirement of such materials is the hot stage blades in a gas turbine. The desired properties in this case are high temperature and corrosion-resistant. The solution is to provide the strength from core bulk and corrosion resistant on the surface. This can be obtained by coating a corrosion resistant material on a material that can sustain higher temperatures. The coatings are desirable for many other reasons including economics, material conservation, unique properties, and design flexibility.

This surface coating is obtained by depositing a coating onto a substrate by processes such as physical deposition, chemical vapor deposition, electro deposition and thermal spraying etc. Thus, the coating/substrate is a composite materials system. The properties of the composite material depend on the properties of the two components and also on the interaction between them. The composite material can be of two varieties. In one the coating and the substrate are two different materials. This is usually formed by overlay coating. In the other variety, the surface is the combination of both substrate material and the coating material. These materials are usually formed by ion implantation or diffusion coatings.

Before the advent of deposition techniques most solid metallic and ceramic materials were produced by melting or solidification technology. Since the advent of deposition techniques, the diversity of materials that can be produced has increased phenomenally. A much variation in microstructure is possible with vapor source materials. A large number of materials are used for coating. Thin films have been in usage for a longtime. As early as seventeenth century thin films were used in various areas like glass decoration and metallurgy. Suspension of silver salt is used as paint on the glass vial. It was then heated to convert the salt to metallic silver. Another old technique is beating the metals like gold make thin plates of the metals used in various walks of life [56].

The mechanical properties of thin films vary from those of bulk material. Thin films exhibit higher strengths when compared to bulk materials. Properties also vary based on how the metals are worked on. For example, strength of thin films is higher than the bulk materials that were well annealed. These annealed bulk materials have higher strengths when compare to severely cold worked bulk materials. There are two reasons for exhibiting such difference in strengths. First, in annealed materials the crystals are more disordered resulting in smaller grains compared to cold worked bulk materials. The second explanation is that, if the films are sufficiently thin, the dislocation of grains could extend throughout the surface and locked in place, thus giving no mechanics for yielding [56]. In the electronics field, thin films are occupying a prominent place due to their influence on the properties of electron. The addition of thin film can largely influence conductivity and resistance properties of a material. In thin dielectric films the conductivity abruptly changes when the thickness is reduced below a finite amount. In dielectric films that are thicker than 100 A, the field required for current flow is independent of film thickness. In thinner films the density of current increases considerably. The reason for this increase is the

“Tunneling’ effect caused by decrease in thickness. The probability of an electron to penetrate a surface represented by dielectric, and it increases with the decrease in thickness [13].

Many fields are experiencing the advantages of thin film coatings. The use of thin films in optics began in nineteenth century. Around this time, it was observed that tarnished lenses are better than the clear ones. This led to further research and as a result, in 1930’s it was detected that the higher transmission in the tarnished lenses is because of interference phenomenon. This has resulted in developing coating on lenses. This was used for numerous applications like preventing light loss, reduction of unwanted light in optical image, and removing images of sky on World War II plane’s instrument, making them more readable. Another prominent thin film used in modern era is the magnetic film. The need for magnetic film arose to aid the development of high speed computers with large memory capacity. Earlier computer memory consisted of magnetic drums. These drums have many limitation when it comes to speed and storage capacity. These limitations were overcome by using the magnetic films for storage. Replacing magnetic drums with films containing some perm alloys made this possible. These films below certain critical thickness show magnetic direction reversal time less than 10^{-9} seconds. Typically, these films consist of 80 percent nickel and 20 percent iron. This is also very inexpensive which allows larger memory at a smaller price compared to magnetic disks. In electronics, early film resistors were created using a resistive consisting of carbon. One of the first film resistors was made by spraying platinum on a glass rod. The resistance of the films depends on their geometry and structure.

2.2 Thin Film Deposition Techniques

Thin film Deposition techniques are constantly evolving. There are many deposition techniques for material formation [22-25]. Broadly these techniques can be classified in to two major areas namely physical techniques and chemical techniques. The chemical reaction involves in chemicals directly reacting with substrate and forming the deposition. This method may also result in formation of other compounds in the form of vapor or gases. The physical reaction does not produce byproducts. There are considerable numbers of techniques that are based on both physical and chemical reaction [61]. Following are some of the popular deposition techniques [62-64].

- Electro-deposition
- Chemical Reduction
- Electroless Plating
- Vapor Plating
- Evaporation
- Sputtering
- Anodization
- Polymerization

Among these deposition techniques, our project's focus is Chemical vapor deposition. From here on we refer to this technique as CVD.

Chemical Vapor Deposition (CVD)

In this process, the thin film substrate is placed in a chamber and gases are released into the chambers. A chemical reaction takes place between the primary gases in the chambers. This reaction results in formation of a solid material that condenses and falls on the thin

film substrate as a coating on the surface. The reaction of primary gases is the main difference between CVD and other physical deposition techniques [61-64]. The development of the CVD process was mainly due to growing practical needs of society. One of the most important applications of CVD films is for electronic field. This method is very useful in fabrication of thin film transistors, resistors, sensors, capacitors and solar cells. Successful growth of any material is affected by the properties of the layers grown. Controlling these properties depends on the parameters and conditions of chemical reaction. Better understanding of these chemical layers is very important to produce improved quality layers. CVD is a complex process involving fluid mechanics, heat transport, multicomponent diffusion, gas-phase chemistry, surface chemistry and crystal growth.

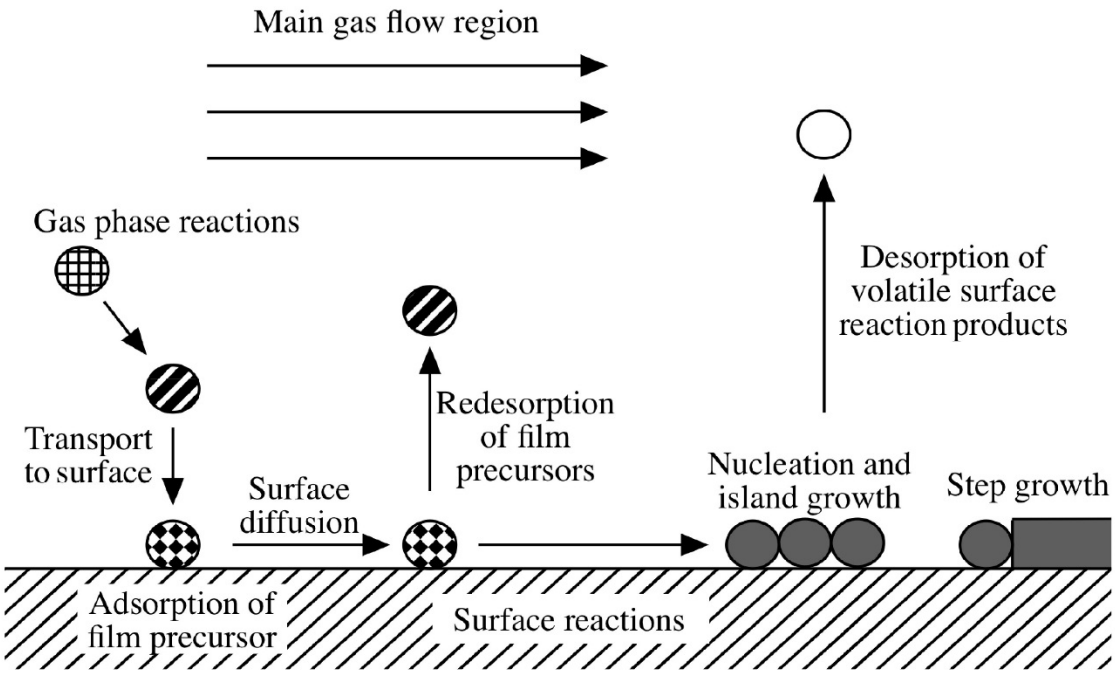

Figure 4: Illustration of fundamental transportation and reaction processes underlying CVD [64]

The deposition sequence can be summarized in to following steps [64].

1. Gas flow through main gas flow region from reactor inlet to the deposition zone.

2. Gas phase reactions leading to formation of precursors and byproducts.
3. Transportation of precursors to the growth surface.
4. Collection of film precursors on the growth surface.
5. Surface diffusion of film precursors to growth sites.
6. Incorporation of film constituents in to the film.
7. Desorption of byproducts of surface reactions.
8. Mass transport of by products from deposition zone towards the reactor exit.

Each step of the process must be controlled in order for CVD to accomplish uniform composition and thickness of thin film. Apart from this the reactor should be designed and operated to accurately control crystal structure, surface morphology, and interface composition. There have been several studies revealing fundamental dynamic effects (e.g., shadowing, re-emission, surface-diffusion, and noise effects) taking place during the growth process [65-69]. Studies towards explaining the growth dynamics have been partly successful and only the simulation-based studies were able to include all these effects.

In our work, the main focus is on how the re-emission and shadowing will affect the growth process and will affect the surface morphology of substrate. We believe that by using computer network modeling, these effects can be explained and understood much better. This would facilitate scientists to develop models to control these effects to attain required growth and structure of thin films.

2.3 Monte Carlo Simulation

Monte Carlo methods have been used since the second half of the nineteenth century, but only in the past few decades have the technique gained the status of a numerical method

capable of addressing the most complex applications [70]. The Monte Carlo method is designed to solve problems consisting of many independent smaller ones (like the spin of a roulette wheel, or toss of dice at a casino), using a random number generator. Its core idea is to use random samples of parameters or inputs to explore the behavior of a complex system or process. The method's name was adopted from the Monte Carlo casino which was one of the best-known venues for roulette and games of chance in Monaco. The fair roulette wheel is one of the earliest random number generators. The use of randomness and the repetitive nature of the Monte Carlo process are analogous to the activities conducted at a casino. Monte Carlo methods formed the core of the simulations required for the Manhattan Project. Applications resulting from this project included the design of shielding for reactors [70]. The Monte Carlo method provides solutions to mathematical problems by performing statistical sampling experiments on a computer [71,72].

The main components of the Monte Carlo method are [73]:

- The probability distribution functions describing the physical system.
- The random number generator which is a source of uniformly distributed random numbers.
- The sampling rule which is a recommendation for sampling the probability distribution function.
- The variance reduction techniques, which are methods for reduction of the computational time for Monte Carlo simulation;
- The scoring (or tallying), which represents the outcomes of the interest quantities.

Monte Carlo simulation serves as a better modeling technique for film growth using CVD technique. The film growth has statistically extensive computations which are proved to be handled accurately by Monte Carlo Simulations.

2.4 Network Modeling

In late nineteenth century biologists and physicists have started taking advantage of each other fields to find solutions and explain phenomenon in their respective field. As both the fields started to grow enormously, basic theories and concepts in their fields were not sufficient enough to answer the new challenges emerging in these fields. They started to look at other fields for the answers. For example, the need of high quality microscopes for biologists has motivated physicists to improve microscope technology [74]. Advent of computers has helped physics among other disciplines to move outside their traditional approaches and explore more statistically challenging systems. Some of the behavior is not easy to explain using laws of fundamental particle interaction. Many systems exhibit complex, unpredictable, and chaotic behavior at global level. Even though such systems are chaotic at global level, they consist of simple individual interactions. Computers have provided them the computational power and large data sets to explore various methods to capture behavior of a system. These large datasets are allowing scientists to study real networks that consist of millions of nodes [75]. The well-established component of mathematics, the graph theory allows researchers to model the systems in to networks and study their characteristics both locally and globally.

2.4.1 Graph Theory

In mathematical terms a network is denoted as a graph. *A **graph** G is a pair of sets (V, E) where V is a non-empty set and the elements of E are pairs of elements of V*. If the elements of E are ordered pairs denoted as (a, b) then G is called a directed graph (digraph). If the elements of E are unordered pairs denoted as {a, b} then G is called an undirected graph.

The following are the pictorial representation of simple graphs. The vertices *(V)* are represented by the dots. The edges *(E)* are represented by the lines connecting the vertices.

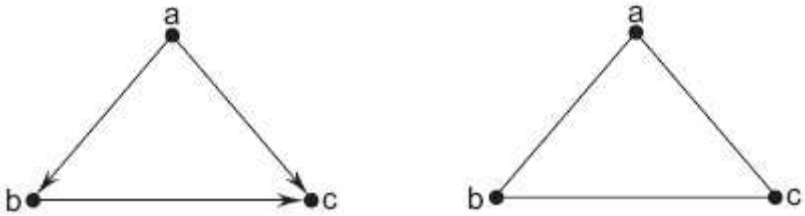

Figure 5: *(a) Directed Graph* *(b) Undirected Graph*

In an undirected graph, the number of edges connected to each vertex is described as the degree of that vertex. The degree is denoted as k. In a directed graph, there are two varieties of degrees. The number of incoming edges is called in-degree and is denoted as k_i. The number of outgoing edges is called out-degree and is denoted as k_o. Thus $k = k_i + k_o$.

Another important aspect of graph theory is path. A path is a non-empty graph P= (V, E) of the form $V = \{x_0, x_1, x_2, x_3 \ldots x_k\}$ and $E = \{x_0x_1, x_1x_2, x_2x_3, x_3x_4 \ldots x_{k-1}x_k\}$, where x_i are all distinct. x_o and x_k are linked by P and are called its ends and $x_1, x_2, \ldots x_{k-1}$ are called its inner vertices. The path is referred as sequence of its vertices, writing $P = x_0, x_1, x_2, x_3 \ldots x_k$ and call P a path from x_0 to x_k. This can also be called as path between x_0 and x_k [76]. The length of path is number of edges that constitute the path.

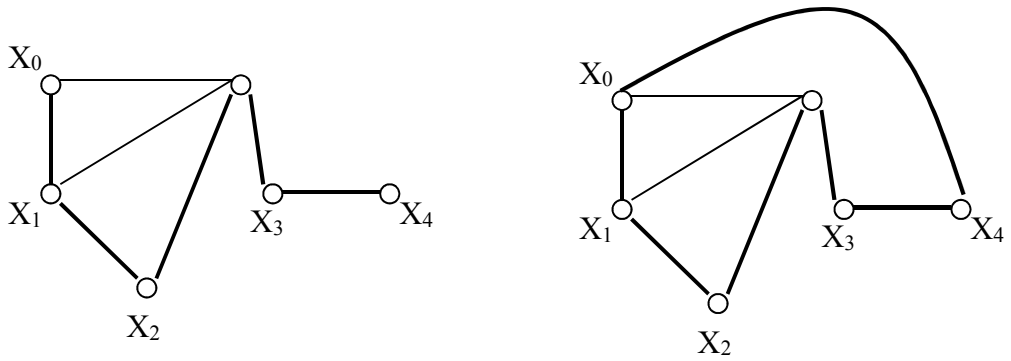

Figure 6: (a) Non-cyclic Graph (b) Cyclic Graph

In the Figure 6(a), if the thick edges connecting the nodes $X_0 \ldots X_5$ is the path then it is written as $P = X_0, X_1, X_2, X_3, X_4, X_5$ or $P = X_0, X_1 \ldots X_5$. The length of the path is 5. In figure 6(b) the edge X_4X_0 is also part of the path and the path has same starting and ending vertex. This is called a cycle. If $P = X_0 \ldots X_{k-1}$ and $k \geq 3$, then the graph $C: = P + X_{k-1}X_0$ is a cycle. For cycles, we denote their paths with cyclic sequence of vertices. For figure 6(b) the cycle is written as $C := X_0X_1 \ldots X_4X_0$. A graph without loops is called a tree. If a tree does not have separate parts then it is known as connected tree. In a connected tree the number of vertices (N) is greater than the number of edges (E) by one. N =E+1. In figure 6 we have 8 nodes whereas the number of edges is one less than the number nodes (7). Since there are no disconnected parts, this is a connected tree. An undirected graph is called bipartite if it has two distinct sets of nodes U and V such that every edge connects a node in U and V and is written as G = (U+V, E).

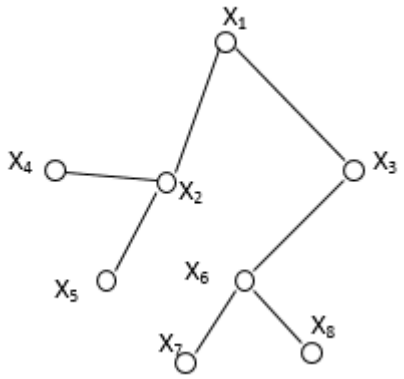

Figure 7: Connected Tree

Reachability of different nodes is an important component of graph theory. Many features of graphs can be studied based on reachability of different nodes. Reachability is the possibility of a path between two nodes. This path could be an edge between the two nodes or could involve multiple nodes of the graph.

The vertices are not universal. They differ based on the type of networks being studied. For example, in a friend network a node representing a person can be classified based on age group, gender, their associations like college attended, college majors etc. These classifications allow scientists to study the local properties of the graph as well as global properties. When studying a friendship network of university students, classification of nodes can bring more useful information like probability of friendship between different majors or probability of friendship among different economic classes etc. It is very important to recognize the characteristics of nodes that one has to use while studying a network. By not classifying the nodes properly, scientists will miss out important behaviors of the networks. Another challenge in studying networks with large data sets is to acquire a complete and unbiased set of data. This could be due to amount of time it takes to gather such information, limitation of tools, technologies, methods or other available resources.

2.4.2 Network Properties

The analysis, discrimination and synthesis of complex networks rely on measurements that could represent the relevant topological features [13]. Numerous studies have been carried out to study the dynamics and measurements of the networks. Among these there is a particular focus on networks derived from real data involves community structure, degree distributions, and hubs. These are studied along with various existing models of networks like small-world [77-79], Scale-free models [80-82], and community structures [83-84]. The quantitative analysis allows us to classify the real networks into major categories, thus allowing us to focus on particular theories and analysis in their study. An additional component called transformation can be introduced in studying these networks. This is essential in analyzing evolving or dynamic networks. For example, one can compare the

measurements or characteristics of networks over a period of time and determine how the network has changed over that period. A network can be compared to its initial stage and after removing some prominent nodes or hubs removed from the network. These investigations give insights on both original state network and transformed network when right measurements are chosen.

In the followings, some popular network measurements are reviewed.

Shortest Path Length: In a graph G, the distance between two vertices u and v is the length of a shortest path joining u and v and is denoted by d_{ij}. If two nodes are directly connected by an edge, then the shortest path length is 1.

Average Shortest Path Length: In a connected graph G, the average distance of G is the average over all distances d(u; v) for u and v in G. If G is not connected, we determine the average distance to be the average among all distances d(u; v) for pairs of u and v both belonging to the same connected component.

$$l = \frac{1}{N(N-1)} \sum_{u \neq v} d_{uv} \qquad (1)$$

The average shortest path length is also called Characteristic path length. In some literature, it is also referred as size of the network.

Diameter: The diameter of G is the maximum distance d(u,v) where u and v are in the same connected component. The diameter is the longest of all shortest path lengths among all possible pairs of nodes.

Density: The density of a graph is defined as the ratio of number of edges in the graph to the maximum number of edges possible for the nodes in the graph. The graph is said to be

dense if these numbers are close. The opposite of dense graph is sparse graph. In a sparse graph, there are only few edges compared to maximum possible edges. Graph density is defined as:

$$D = \frac{2|E|}{|V|(|V|-1)} \quad (2)$$

Vulnerability: In a network topology, it is important to know which components are important for the network's functioning. Many networks have hubs which are heavily connected to other nodes in the network. In many networks these hubs are very important for proper interactions between nodes. But this is not necessarily true in all networks. For example, in WWW network removing hub will drastically change the network. But in a binary tree where hubs are absent, root and nodes near the root are more important compared to leaf nodes. Disconnecting or deleting these prominent nodes will have dramatic impact on whole network. A way to find critical components of a network is by looking at these nodes. Vulnerability of a node is network efficiency variance before and after the node and all its edges are removed [85]. Network vulnerability is calculated as maximum vulnerability for all of its vertices.

Degree Distribution: The degree distribution of a network P(k) is the probability of a randomly selected node having degree k. Degree distribution is calculated by counting number of nodes in the network, N(k) with k edges. This number is then divided by total number of nodes in the network, N. For a directed graph, similar method is used to calculate the in-degree and out-degree distributions. Instead of total number of edges only In and out bound edges are used in the calculation. The degree of a node is a local measurement. By using degree distribution, this local measurement is used to describe the global properties

of the network. In a random network the probability of existence or non-existence of an edge is same. Hence the degree distribution of a random network is poisson distribution. Seldom the real-world networks possess this property [86].

Clustering Coefficient: The clustering coefficient is a measure that provides insight to the connectivity of a node's neighborhood in a network [86]. The equation for clustering coefficient is

$$(C_i = 2E_i) \,/\, k_i(k_i - 1) \qquad (3)$$

where E_i is the number of edges connecting the immediate neighbors of node i, and k_i is the degree of node i. Average clustering coefficient is calculated by averaging the clustering coefficients of all nodes in the network. Most real-world networks exhibit large average clustering coefficients. Large average clustering coefficient indicates high level redundancy and cohesiveness. The average clustering coefficient of nodes with degree k can be plotted as a function of node degree, $C(k)$. It has been found that for many networks, this clustering-degree relation has the functional form.

$$C(k) = Bk^{\beta} \qquad (4)$$

In the above equation, exponent β is usually between 1 and 2. By starting at an edge of a given node and following a *path* along connected edges [64, 76], only some of the nodes in the network will be connected to the starting node. Often in directed graphs, the possibility of two edges being consecutive depends on their directions. If every pair of nodes in a network has edges connected between them, then the network is said to be strongly *connected*. The *average path length d* is the average number of edges in the shortest path between any two nodes in a network. This global property of a network is

used to understand the schematics of a network. For most real-world networks the average path length is seen to increase / decrease with the number of nodes in the graph:

$$d \sim ln(N) \qquad (5)$$

If the path length is small even when the networks become large it is said to be displaying the small world property [86]. Studying global efficiency of a network is very important in directed graphs. The path length between unconnected nodes is infinite. Such nodes do not interest researchers trying to gauge the global efficiency. For this detection of communities among these graphs and studying these communities will provide invaluable information about various actors in the graph.

For example, many communities exist in a directed graph. These communities are generally strongly connected and are connected to other communities or subgraphs through an incoming or an outgoing edge. By community detection and the way they are connected with other portions of graphs will provide insights on how the network is organized and the complexity of the network.

2.4.3 Network Models

Random Graphs: Pal Erdős and Alfred Renyi has pioneered a well-developed branch of mathematics called random graph theory. To analyze any graph that appears to have random topology, researchers rely on random graph theory. While analyzing a complex network, one compares the properties and behavior of the network to a random network with same number of nodes and edges. ER random graph theory captures the qualitative topology changes when number of nodes and edges are increased in a graph. An ER graph is formed by randomly forming edges E between N number of nodes. The degree

distribution of a graph follows a Poissonian distribution. Most nodes have degree distribution closer to average degree of the network, k.

$$< k >= 2E/N \qquad (6)$$

Most real networks have scale-free degree distribution. But ER random graphs have homogeneous degree distribution. The average clustering coefficient of ER graphs is inversely proportional to the size of the network. Clustering coefficient of these graphs is given by

$$< C >=< k > N \qquad (7)$$

and the clustering coefficient is degree independent in ER graphs, peaking at the connection probability p. In real-world networks the clustering coefficient is high and is inversely related to degree. The average path length of ER graphs is given by equation (8).

$$d >> ln(N)\, ln\,(k) \qquad (8)$$

In this case d remains small, even when the network is large [15]. Many real-world networks have average path length similar to those of random graphs with same number of nodes and edges. There are some well-known networks like World Wide Web that have considerably longer average path lengths.

Scale-Free Networks: Derek de Solla Price gave the first example of a scale-free network. He studied the citations network between scientific papers and found that both in and out-degrees display power-law behavior [19]. Price published another paper some years later [65] in which he offered the explanation for power-law degree distributions which was built on ideas developed Herbert Simon [124], who showed that power laws arise when "the rich get richer," when the amount you get goes up with the amount you already have. In sociology, this is referred to as the Matthew effect [67]. Price called it cumulative

advantage. Barabasi and Albert calls this preferential attachment. [23]. Prince took Simon's idea of wealth distribution and applied it citation network behavior. Price in his paper explains that the rate of increase in citation are proportional to the citations already exists for that paper. The probability that a newly appearing paper cites a previous paper—is simply proportional to the in-degree k of the old vertex. Since each vertex starts with in-degree zero, and hence would forever have zero probability of gaining new edges. To address this problem, Price suggests that the probability of attachment to a vertex should be proportional to $k + k_0$, where k_0 is a constant. Although he discusses the case of general k0, all his mathematical developments are for $k_0 = 1$, since one can consider the initial publication of a paper to be its first citation. Thus, the probability of a new citation is proportional to k + 1. The probability that a new edge attaches to any of the vertices with degree k is thus illustrated by following equation [7].

$$\frac{(k+1)P_k}{\sum(k+1)P_k} = \frac{(k+1)P_k}{m+1} \qquad (9)$$

Barabasi et al. also examined similar preferential attachment behavior in WorldWideWeb network. These networks display the long tail distribution phenomenon [24].

Small World Networks: Social scientists studied this phenomenon pioneered by the work of Stanley Milgram in 1967. Milgram showed that the chains of acquaintances linking a pair of Americans appear to have length six on average, leading to the phrase "six degrees of separation" between any two people in the U.S. [18]. Recent work by Dodds et al. suggests it's still true [17]. In his original basic experiment, Milgram managed to relay a message from a source person in Nebraska and to a target person in Boston such that the chained people (who had received the message) needed to forward the message to someone they knew on a first-name basis and who are either closer to, or was more likely to know, the target.

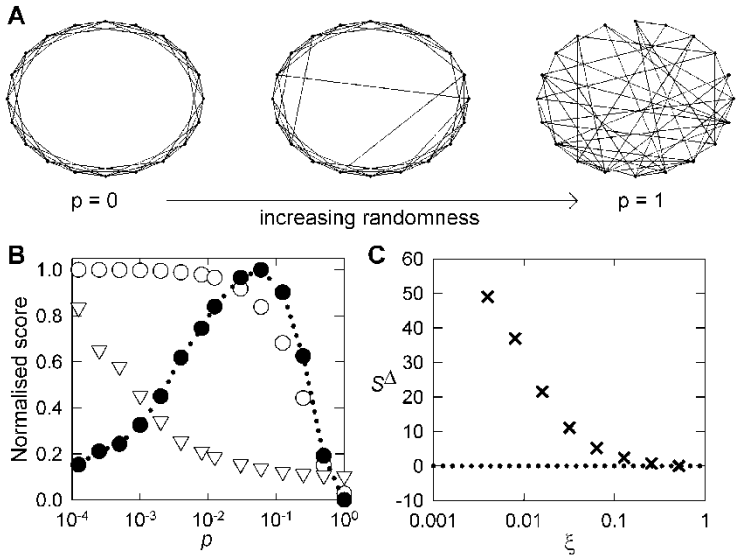

Figure 8: Watts-Strogatz (WS) small-world network model. [120]

The small-world network "displays considerable local connectedness while also having a low degree of separation with the other nodes in the network" [120]. Many real-world networks, including some social networks, have displayed to the small-world network construct.

In our network model, with valleys and peaks forming over a time period, the particles travelling between them might show some degree of small world behavior. Theoretically this behavior might be demonstrated when the number of clusters decrease significantly at higher sticking coefficients. It would be interesting to see how the local connectedness exists at lower sticking coefficients, where the number of clusters is very high. In our work, we study if the dynamic growth of the network displays any properties of small world graphs. The network G is said to be a small-world network if the graph has similar path length as of a E-R random graph ($L_g \geq L_{rand}$) and has greater clustering coefficient than the E-R random graph ($Cg >> C_{rand}$) [120].

2.5 Applications of Networks

Networks are present in many aspects of our world. Study of such networks has become one of rapidly growing research areas. These networks are compared, analyzed for various mathematical and topological properties. Such studies are highly interdisciplinary. Our existence depends on many of these complex systems. Understanding systems such as power grids, disease epidemics, transportation systems etc. are essential to our survival. It is important to study failures and their cascading effects of many components in such systems.

NETWORK	NODES	LINKS	DIRECTED / UNDIRECTED
Internet	Routers	Internet Connections	Undirected
WWW	Web pages	Links	Directed
Power Grid	Power plants, transformers	Cables	Undirected
Mobile-Phone Calls	Subscribers	Calls	Directed
Actor Network	Actors	Co-acting	Undirected
Citation Network	Papers	Citations	Directed

Table 1: Various Network maps and their nodes and links [103]

In the event of local failure, the load can be shifted and reorganized to other nodes without causing a cascade affect. Many complex networks suffer from cascading failures. Care should be taken to reroute the load. The cascading failures take place on the Internet, when load is rerouted to avoid non-responsive routers. This rerouting may occasionally create denial of service attacks on routers, if they are not equipped to handle the extra traffic. We

must understand how network topology affects the functioning of complex networks. In this section, we will look at some frequently studied categories of real-world networks.

2.6 Network Traffic Modeling

Design and study of traffic models shed light on patterns, characteristics, and behavior of the traffic. These insights are used to design and implement more robust and high-availability networks. There has been a significant interest in traffic models and its behavior since Self similarity and Long range dependency has been discovered [134]. In recent times the volume of data has increased phenomenally that has intrigued researchers to find more efficient models to study, characterize and predict the traffic and the network as a whole. The aim of traffic modeling is to find stochastic processes that would capture the traffic behavior of the system under study and is universal and scalable. Main components of a traffic model are nodes, edges established between these nodes, Queueing method and the packets travelling between the nodes through the edges. During an active session, an edge is established between two nodes and the packets are transmitted. The transmission of these packets is called flow of traffic. The flow could have different characteristics. For example, it could be continuous or discrete. In a traditional queueing models the traffic follows a continuous flow. Whereas the Internet traffic is a series of little bursts where the traffic can be heavy at certain times compared to others. Each burst consists of transmission of set of packets in a small interval of time. It is observed that in the Internet traffic, flow of packets for a very long period is scarce.

There are many models available in literature. Some of the popular ones are:

1. Poisson Distribution Model

2. Pareto Distribution Process
3. Weibull Distribution Process
4. Regression Models
5. Fractional Brownian Motion
6. Markov and Embedded Markov Models

We cover a few of these traffic models below.

Poisson Distribution Model: Poisson distribution is one the earlier models that was used to study the traffic. This was a prominent model to study the traffic for telephonic systems [138]. This is a memory less and independent of prior arrival times. The next arrivals are exponentially distributed and do not take account of earlier arrivals. The number of arrivals have Poisson distribution in any given interval of time [135]. This model is very attractive because of its independent memory less behavior. Another property that makes Poisson calculations simple and neat is that

Self-Similar Traffic Models: Poisson method is suitable to study traditional traffic. But, bursty traffic like the Internet traffic is studied using Self-Similarity models. In recent years since Leland et al. observed the burstiness of the Internet traffic, researchers are considering Self-Similarity study necessary for traffic modelling. Self-Similarity is long-range dependent compared to short dependency nature of Poisson model. Heavy tailed distributions can describe self-Similar process [95-99]. Researchers have found self-similar model to be very narrow and difficult to implement to study the traffic. As an alternate they prefer a different version of self-similarity called asymptotically self-similar model [75]. Autocorrelation function of asymptotical self-similarity process can be defined as follows

$$r(k) \sim ck^{2H-2}, k \to \alpha \qquad (10)$$

where H is Hurst parameter and c is a constant greater than 0. Fractional Brownian Motion is an actual Self-Similar model whereas Fractional Gaussian Noise is exactly asymptotic Self-Similar traffic model and is considered to be a good model to study Ethernet, Telnet and FTP traffic [100].

ON-OFF Model: A simple ON-OFF model has two states where the source is in idle mode or active mode. In a telephone traffic model, a person is either talking or listening. Similarly, in computer network model, a source will either transmit the packets or receive the packets.

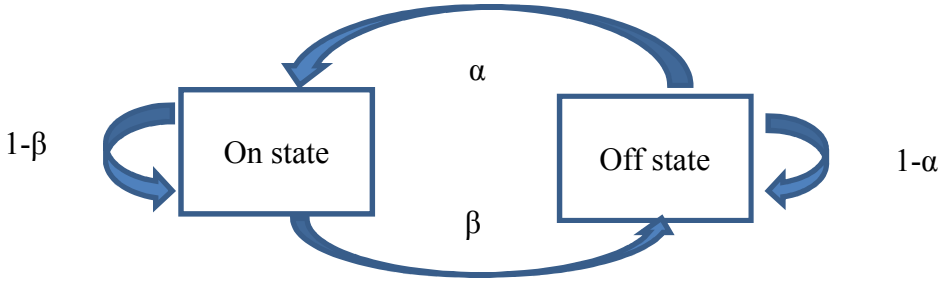

Figure 9: ON-OFF Traffic Model

Once the source is in on state, the model generates packets at constant rate for a period. It then transitions to off state at transition rate of β. It then stays in off state before transitioning to on state at a rate of α. This model is used when it is desired to capture the scaling behaviors of the network traffic. It was used to study the IP traffic, but later studies showed that a simple ON-OFF model is unable to capture the statistical and long-range patterns of the Internet traffic.

Autoregressive Models: Autoregressive model is a simple time series model. In autoregressive models, the traffic output is predicted by using previous outputs and inputs.

There are several variations of this model. If the models use only previous outputs they are called autoregressive models. If the models use only the input to predict the output, they are referred as moving average models [101]. Each point in these processes is a linear combination of previous points.

Application Specific Models: There is no one universally accepted model that can be used to study the traffic processes. There are many models that are based on specific application or the nature of traffic. Usually they are variants of some of the models mentioned above. These models are built to capture the true nature of real-world application traffic. For example, some of the popular application models studied are Web traffic, peer-to-peer traffic, and multimedia streaming. It is estimated 40 percent of traffic is Web based [102]. It is possible to apply time series models to study the Web traffic. Since Self-Similarity was already found on the Ethernet traffic, it is logical to look of similar process in Web traffic. It was determined that Web traffic exhibits Self-Similarity characteristics with a Hurst parameter between 0.7 and 0.8. It is also found that web clients exhibit ON-OFF characteristics [103]. This shows that many models can be used to study the traffic processes.

The intricacies of the underlying drivers for traffic models make it tough to choose one model over another. No one model will fit for all kinds of traffic studies. Many factors in real network traffic data will determine the choice of the models to be used. Traffic behavior like Self-Similarity, long range dependency (LRD), fractals have significant impact on the performance of the network. The practical difficulty in modeling real-world traffic is collecting and analyzing large sets of data without any interference. The end goal will also drive the model choice. For example, some models are better equipped to analyze

packet level traffic where as other are more suitable to analyze high level data at nodes, sources, and routers. The chosen model should provide universality, scalability and should be able in line with actual traffic statistically. Our knowledge about the network traffic comes from observing historic data and this influences our ability to predict the future traffic accurately. Traffic model should be mathematical approximation of actual traffic behavior [94]. Many studies have focused on increasing forecasting accuracy by using various methods. Recently some scholars have developed complex networks to explore traffic dynamics. Tang et al. [104] proposed that using complexity and periodicity in complex networks will improve the predictability accuracy.

Chapter 3: Modeling Thin Film Growth as a Network

3.1 Modeling Dynamics of Thin Film Growth

Thin film growth is a complex phenomenon that forms hills and valleys. Two important phenomenon in thin film growth are shadowing and re-emission effects. Non-local interactions on the surface of a thin film growth originate from shadowing and re-emission effects. These interactions can lead to trajectories of atoms/molecules before they are finally deposited. For example, during re-emission, when an atom bounces off a point and lands on another, the points can be treated as nodes and path between them as an edge between these two nodes. when the sticking coefficient is small, the particle can go through multiple hops landing on various surface points and forming multiple edges. With shadowing effect hills are more prominent and act as first landing spot for the atoms on the surface. This is similar to nodes with high traffic in a network.

Several factors need to be considered while mapping surface points and the parts followed by atoms to a network modeling framework. Figure 10 shows the depiction of hills and valleys on a thin film. In Figure 10(a), the blue color represents hills and yellow color represents the valley of the film. The first thing in modeling is to define a “node” in the network framework. Each blue or yellow region on the film should be mapped to a network node. The resolution of the grid determines the position and number nodes used for modeling the network. If the grid resolution is too fine, then each point on the surface of thin film is treated as a node. Thus, a blue/yellow region of the film will contain multiple nodes as in Figure 10(b). Conversely, when the resolution is coarse, then blue/yellow regions on the thin film surface will be mapped as one network node as in Figure 10(c). Finer grid is more likely to capture local interactions and other dynamics of the growth

pertaining to the *re-emission effect*. On the other side, the coarser granularity network models enable us to observe uniform behaviors pertaining to the *shadowing effect* in the film growth dynamics [55]. This has been discussed in detail in chapter 4. This intuition derives from the fact that re-emissions take place from an atom-size starting point to another atom-size ending point on the surface, whereas shadowing happens because of hills with significantly larger sizes than atom-size. In our first method, we developed a finer granularity network model to capture the re-emission effect's uniform behaviors and then apply clustering techniques transit to coarser granularities for capturing the shadowing effect's uniform behaviors. The importance of granularity on the resulting network model is illustrated in Figure 10, where the grid network model is developed to capture local interactions.

After determining the nodes on the thin film, we then map growth dynamics to corresponding grid network model as shown in Figure 10. During shadowing effect, the hills act as initial points of contact for the atoms. As part of re-emission effect, these atoms are then distributed to lower points in the valleys which act as gathering centers. The emissions can then be modeled as a link between the points the atom has landed. The time delay for particle to re-emit from one point to another can be considered as propagation delay. The capacity of the link can be defined as highest number of particles that can simultaneously travel between nodes. This is dependent on physical space available and average size of the particles.

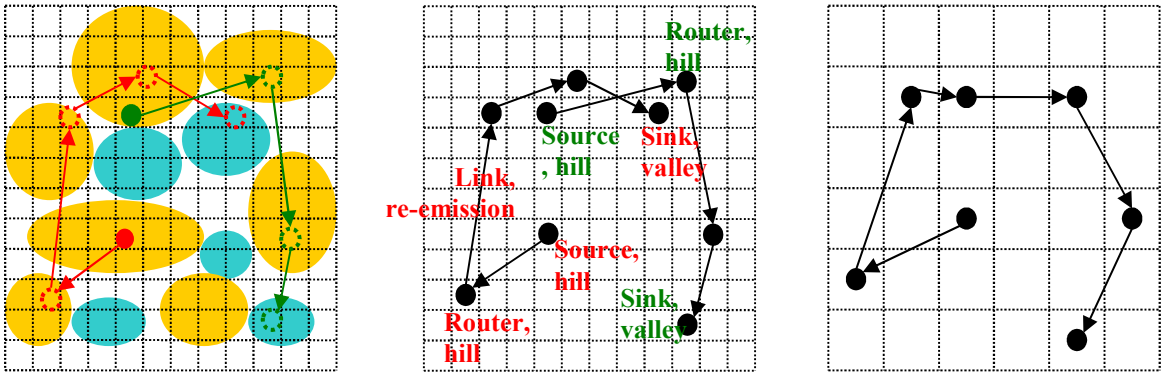

(a) Two particles re-emitting on a growing thin film

(b) Network model in fine space granularity

(c) Network model in coarse space granularity

***Figure 10**: Depiction of Grid network model development. Consider an example of two particles landing on a thin film substrate. The red and green particles go through four and three re-emissions respectively. [21].*

In networking terms the nodes can be classified as source, router and sink. The initial point at which the particle usually lands (in case of shadowing effect, this is usually a point on a hill) is the source. After the redistribution from the hill, where the particles are reemitted before destination are classified as routers. As illustrated in Figure 10, a "traffic model" is constructed by tracking the atoms and their trajectories from a starting point on the film and its ending point. That is, if we consider the film as a grid with two dimensions, the traffic from point (i, j) to the point (u, v) can be measured by the number of atoms initially falling at (i, j) but ending up at (u, v) after several reemissions. This traffic can be modeled at various time-scales depending on the total growth time of the film, so that one can talk about "atoms/sec" as the traffic unit, resembling the "bits/sec" unit in data networks. This approach can reveal the effect of one surface point on the other points, which can be modeled by the "routing" phenomenon of networks.

Also, note that the network modeling framework operates at a particular time-scale. That is, just like network model development over *space* is shown in Figure 10(b)-(c), it is possible to construct different network models in *time* for the same thin film growth

dynamics at varying time-scales. This shows that network-based modeling of thin film growth is very flexible and can capture all possible aspects of the dynamics involved.

3.2 Network Model Development from Monte Carlo Simulations of Thin Film Growth

To develop the network models using the methods discussed in previous sections, we need to track and record the movements of the particles on the surface of thin film. We need to track the source point, points through which the particle is travelling and final destination of the particle. Recording this information is not possible with physical experiment. For this reason, we use Monte Carlo simulation to record the required trajectory information. Monte Carlo method is already shown to mimic the processes involved in experiment and predict precise growth morphology [2].

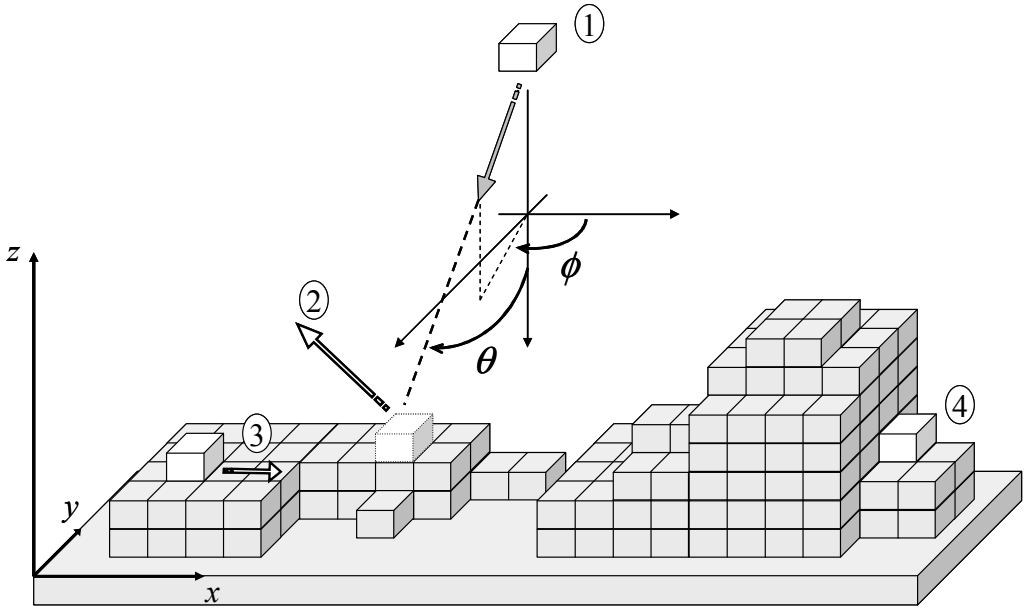

Figure 11: *Depiction of basic steps in the Monte Carlo simulation: (1) A particle is sent towards surface with angles θ and ϕ. The probability of this particle sticking to the surface is s_0. (2) If the particle is re-emitted, it might stick at different point with a probability of s_1. (3) An adatom can diffuse on the surface before it is deposited. (4) Some surface points are in accessible due to shadowing effect and re-emission is not predominant in these locations. [21]*

In Monte Carlo simulation, each particle is considered to be of same size as on lattice unit on the surface of the thin film. As illustrated in Figure 11, depending on which deposition technique is used, an angular flux is chosen. A particle is directed towards a random point on the surface at the chosen angle. Based on the sticking coefficient at the pint of incidence, the particle might go through re-emission and travel through various points before settling at a destination point. At each impact point, the sticking coefficient may vary and is represented by S_n, where n is the order of reemission starting at n = 0. The shadowing effect is included in all emission and re-emission processes. With shadowing effect in place, the atoms travel might be cut short or deviated when they hit a columnar structure that blocks some of the neighboring points on the surface. These points are un reachable to the particle, once they hit the columnar structure or hills. Another important phenomenon through which the atoms move on the surface is through diffusion. When the particle has energy, it diffuses through the surface until the energy is spent or it is overcome by an obstacle on the surface. At this point, the particle is deposited on the surface of the thin film. Figure 11 illustrates various growth processes or steps involved in Monte Carlo simulation method.

3.3 Cluster-Based Network Model

Figure 12 shows the top view images of two surfaces simulated for a CVD type of deposition. It shows image of simulated thin film growth with two different sticking coefficients, 0.1 and 0.9. Figures 12(a) and 12(b) shows the thin film top view. In 12(c) and 12(d), the trajectories of the particles are depicted. In these CVD simulations, the sticking coefficients are kept same for all impacts. In case of larger sticking coefficients, the probability of particle sticking at a particle increase, thus number of re-emissions are reduced. This can be noticed in figures, Figure 12(a), and Figure 12(c). These re-emissions

mainly occur on columnar structures formed due to the dynamic surface morphology of the thin film. In higher sticking coefficient simulations, the formation of hills is prominent and results in increased shadowing effect when compared to lower sticking coefficients. When the hills are formed, they act as collectors of particles coming on to the surface and may distribute them to other neighboring hills. The particles rarely reach the valleys on the thin film. These hills act as nodes in the network being modeled. On contrary, at lower sticking coefficients (Figure 12(b) and Figure 12(d)), particles go through higher number of re-emissions and can connect many surface points. In lower sticking coefficient simulation points in valleys which are usually blocked by hills are also connected because of higher number of re-emissions.

Another interesting observation is that the surface morphology changes dynamically as the deposition grows over time. Figure 13 shows the top view image of CVD simulation for sticking coefficient 0.9. The trajectories are also depicted in the figure. It can be noticed different surface structure is formed at different thicknesses. Thickness of substrate is proportional to growth time. During initial thicknesses, the hills are small and are closer. At this snapshot, the particles move from one hill to another or a valley. At higher thicknesses, the columns/hills will merge together to form bigger columns. Some of the smaller columns that are shadowed by bigger columns will form into valleys. With bigger columns, the particles move from hill to hill and will scarcely travel to valley. This dynamic morphology is dependent on sticking coefficient, angle of incidence of particle, re-emission, and shadowing effect. Change in any of these factors will result in different columnar and valley structures, which will eventually result in different network topology.

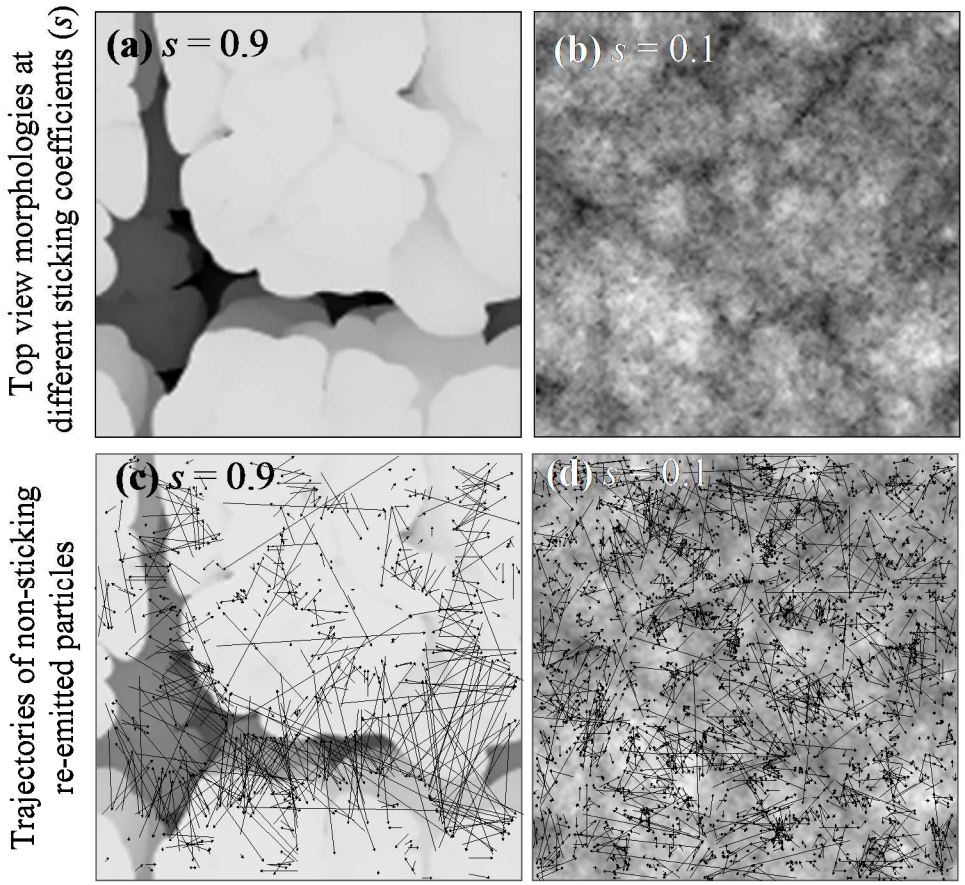

Figure

Figure 12: *Depiction of top view images of thin film surfaces simulated by Monte Carlo method for sticking coefficients a) s = 0.9 and b) s = 0.1. Corresponding trajectories of the re-emitted particles are also mapped on the top view morphologies for c) s = 0.9 and d) s = 0.1. [128].*

Figure 14 depicts the degree distribution P(k) versus degree k of the network modeled after the Monte Carlo simulation. This provides insights to the network characteristics in turn will shed light into the film growth dynamics. The degree distributions $P(k)$ is the percentage of points with "degree (k)". Degree k is the number of links formed due to re-emitted particles in Monte Carlo simulated deposition for various sticking coefficients and various angle of incidences.

The Figure 14(a) and (b) correspond to degree distribution plots of thin film growth at various thickness. Figure 14(a) corresponds to thinner film, whereas, 14 (b) corresponds to

thicker film at a later stage. In these plots, it can be noticed that for different angle of incidences the deposition techniques demonstrates universal behavior which is independent of sticking coefficients and thickness of the film.

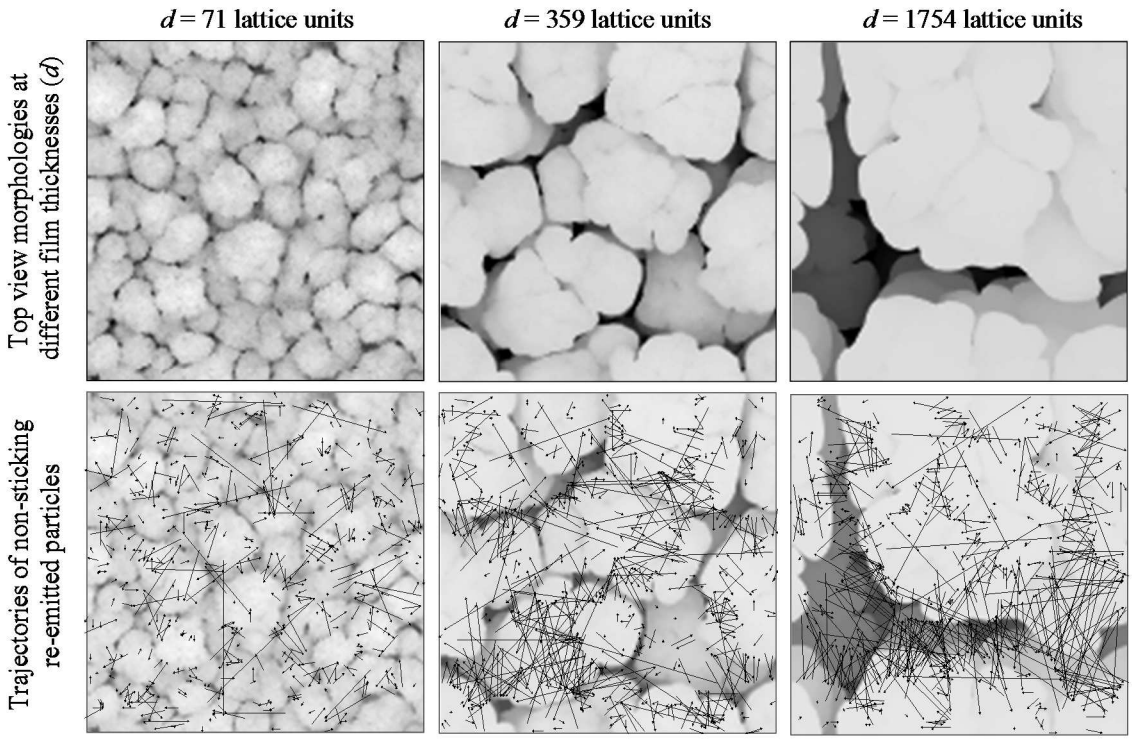

***Figure 13**: First row: Top view images from Monte Carlo simulated thin film surfaces for a CVD growth with s = 0.9 at different film thicknesses d, which is proportional to growth time Bottom row: Corresponding projected trajectories of the re-emitted particles qualitatively show the dynamic change in the network topography. [21]*

The degree distributions for oblique and normal angle seems to be not affected by the sticking coefficients used. This is demonstrated at higher thicknesses in the growth. This leads to different distributions for these depositions. In later stages, oblique angle deposition displays power-law distribution, $P(k) \sim k^2$. These observations suggest presence of universal behavior in angular depositions that is independent of sticking coefficient. Different sticking coefficients produce different morphology of thin film growth. At lower sticking coefficient, the surface is smoother compared to the surface at a higher sticking

coefficient. By being independent of sticking coefficients, we can also conclude that the physical morphology of the surface does not affect this behavior.

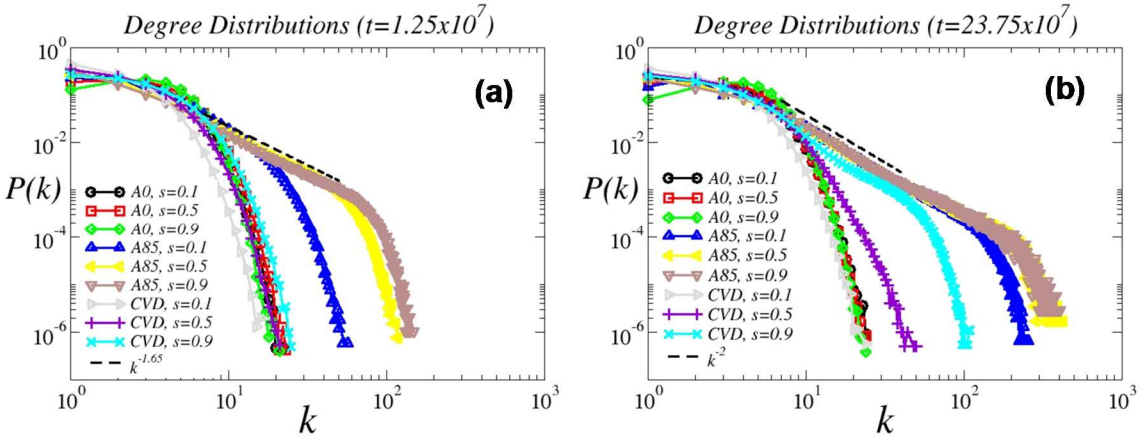

Figure 14: *Behavior of degree distributions P(k) versus degree k for network models of a Monte Carlo simulated normal incidence evaporation (A0), oblique angle deposition (A85), and CVD thin film growth for various sticking coefficients s and for two different deposition time t (left: t = 1.25x10^7 particles, and right: t = 23.75x10^7 particles) are shown. [21]*

The normal angle growth shows an exponential distribution. Whereas oblique angle growth shows power-law distribution. The normal angle growth has re-emission as dominant process and oblique angle has shadowing effect. In line with this observation CVD growth demonstrates exponential degree distribution at lower thickness where the surface is smooth and re-emission effect is dominant. In later stages, it tends to shift towards power-law type distribution.

Chapter 4 Cluster-Based Network Modeling of Thin Film Growth

4.1 Cluster-Based Network Model

We use a cluster-based network model to study the growth dynamics of thin films. As discussed in previous sections, the structure of the surface morphology can be described by hills and valleys. In any network model, identifying the nodes is very important. In this cluster-based method, we treat each column as a "cluster" corresponding to a node of the network. During re-emission, the path between two columns when a particle re-emits from the first point and heads to the second point can define a "network link" between the two columns/clusters. Our network model approach, conceptually, aims to capture these non-random sequences of re-emission.

During thin film growth, we took snapshot images of the film at different thickness values for each sticking coefficient, and we use, i.e., s=0.3 and s=0.9. As for the post-processing, we removed the noise from the images to make them sharper and optimized their brightness and contrast to obtain the cluster boundaries. We determined that boundary detection method along with threshold would be ideal to recognize the clusters in the pictures. Boundary detection is performed by finding the boundaries between objects. By doing this we can determine various objects in the image [105]. By using these methods, we were able to identify the column structures (i.e., clusters) in our images. In Figure 9, the areas inside boundaries are the columns or hills on the film. These columns are considered as the "nodes" of our network model. The size and shape of these columns or nodes change dynamically as the thickness of the film grows.

Although the grid-based model was effective in illustrating power-law patterns in the network modeling of thin film growth, it is not developed in a manner that leverages the specifics of the surface morphology. Since columnar structures emerge as the film grows, particles will naturally bounce between these columns. Hence, we consider these columnar structures while developing the network model.

In Figure 15(a), an enhanced snapshot of the thin film taken from the top view can be seen. The snapshot is taken for deposition with sticking coefficient s = 0.9 at 19 lattice unit thickness. Using Matlab, we have plotted the heights generated by Monte Carlo Simulation. If needed these images are enhanced by adjusting the brightness and contrast using Adobe Photoshop, to make the boundaries thicker and more visible. The clusters are then identified by using an image processing tool called ImageTool [106]. The boundaries of the clusters and the points in these clusters are recorded. The process first involves segmentation of the image into objects and background. ImageTool provides a manual and automatic algorithm for segmentation of the image. After segmentation, the image is converted into a binary image. ImageTool proceeds to identify, count, and number all objects. The areas inside boundaries are the

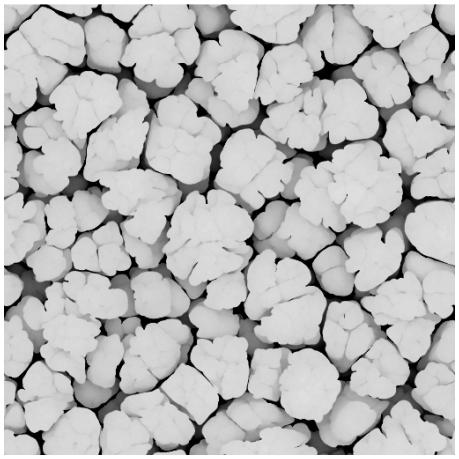

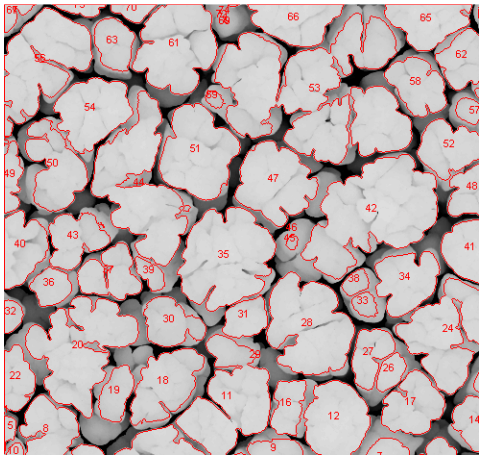

(a) (b)

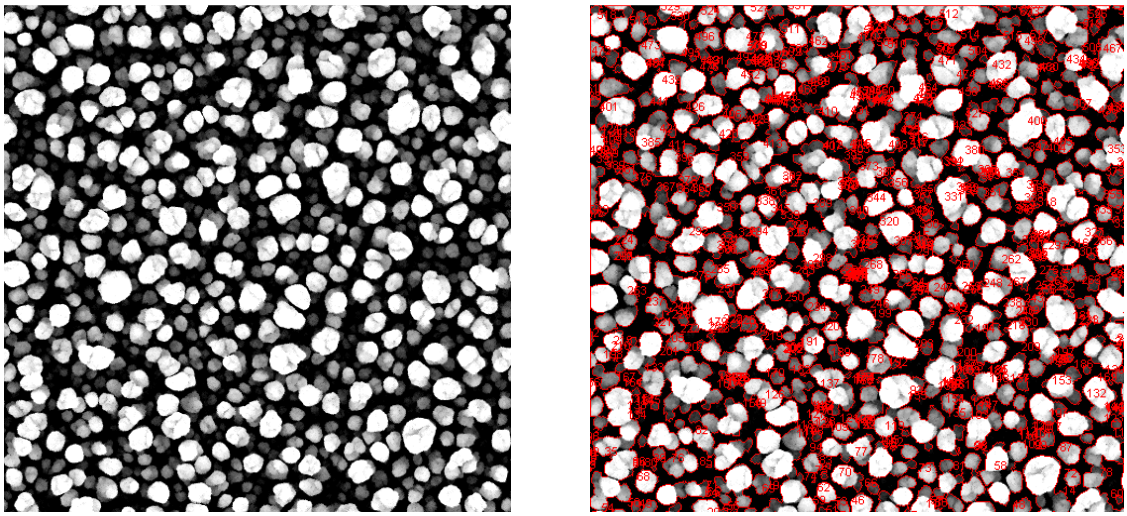

(c) (d)

Figure 15: *(a) (b) Enhanced snapshot and identified columns (nodes) of thin film growth on substrate for following values: So=0.9, depth 19 Deposition Technique. (b) Enhanced snapshot and identified columns (nodes) of thin film growth on substrate for following values: So=0.3, depth 19 Deposition Technique with angle 85.*

columns or hills on the film. Figure 15(b) depicts various columns identified from the snapshot (Figure 15(a)). These columns are considered as the "nodes" of our network model. The size and shape of these columns or nodes change dynamically as the thickness of the film grows. In our previous work, the grid-based model [90], every lattice on the thin film is a node. This does not provide a dynamic property to the nodes in grid model. In the cluster-based network model, the nodes are dynamic; and this helps us better understand the growth dynamics of thin films. We recorded the growth dynamics for various sticking coefficients. We took three samples/snapshots for each sticking coefficient value at various stages of growth. We enhanced the pictures of thin film at these stages to capture better clusters on the lattice. For the initial snapshots, the clusters are very small in size. The size of clusters at this stage is near to the size of individual particles. Each particle

is assumed to be the size of a unit on the lattice. At this time, the model almost resembles the grid model network model where each point on the surface is considered as a node of the network. As time progresses, more and more particles induced on to the lattice group together forming the clusters. In these later stages, significant hills and valleys are formed making the surface rough. After identifying various clusters on the surface, we collect the coordinates of points that fall under each cluster.

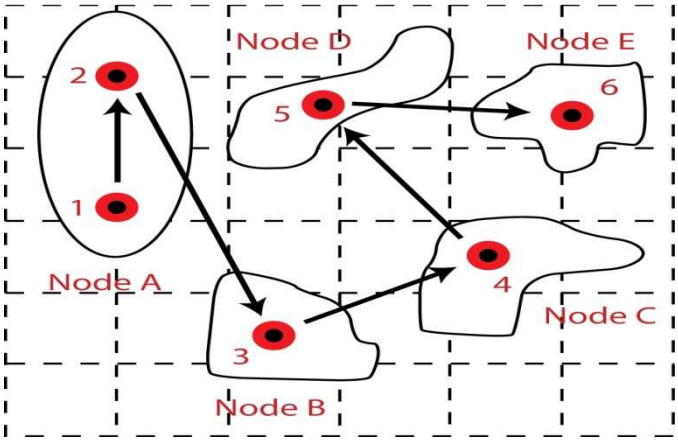

Figure 16: *Trajectory of particle between various clusters*

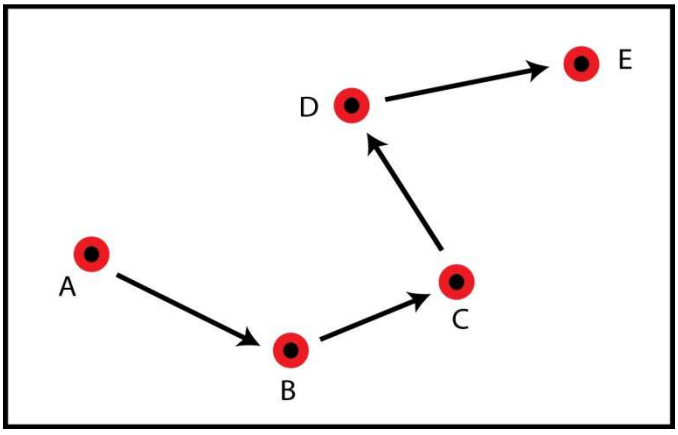

Figure 17: Network representation of a particle trajectory between various clusters.

In the grid-based model the points on the surface are added as nodes to the network when it hosts a particle for the first time. This translates in to the growth of network size. As the

process continues almost all the points are added as nodes to the network. Ideally, all the points are added to the network as nodes. At this stage, the network ceases to be dynamic. With cluster-based model, we extend the dynamism of the network. In initial stages the cluster-based network resembles grid based network. But as the growth process progresses, the cluster-based model ceases to resemble grid model. For a while the network grows as the particles are added to the network as nodes. But in later stages of growth process when the hills and valleys start to appear, the network growth reverses. The number of clusters representing the nodes of the network starts diminishing. As more and more particles descend on to the substrate, the particles tend to fill the gaps between the neighboring columns or hills. In this process valleys act as collecting points for the particles. The particles bounce of the hills during re-emission and settles in the valleys. These areas eventually turn into bigger and wider columns or clusters. Since the number of columns or clusters diminish, the size of network in terms of number of nodes decreases. As the hills grow in the size, they tend to block more particles from reaching their neighboring valleys casting a shadow effect on them. Figures 16-17 represent the re-emission process in terms of cluster-based network model. The black dots represent a single particle at various times during its re-emission. The arrows represent the path or trajectory followed by the particle.

In this model two different approaches are taken to identify the clusters based on which trajectories of particles are mapped. In the first approach, we used the clusters from the snapshot of images at various thicknesses. In this approach, the nodes of the network evolve constantly. In the second approach, we take clusters from snapshot of the image at higher thickness. We assume to super impose these clusters on to substrate surface and then map the trajectories of the particles. In this approach, the nodes are constant throughout the growth process. Each trajectory can be broken down to initial point, routing points, and

final point. We can see that the particle starts at position 1 and after first hop it lands at point 2. The first contact point of the particle with the surface is at point 1. Then it goes on to jump on to points 3, 4, and 5 finally settling at point 6. In this scenario, point 1 is the initial point, whereas points 3, 4 and 5 are routing points and the point 6 is the final point. In networking terms, point 1 is the starting node and point 6 is the destination node. The points 3, 4 and 5 are the routing nodes in between. Based on this, we claim that cluster-based model aptly captures the re-emission effects. This is shown in Figure 16. Since the points 1 and 2 belong to same cluster or node, we represent it only once in the network model.

4.2 Results and Discussions

Figure 18 shows a comparison of degree distributions of the grid-based and cluster-based models, while Table 2 shows the power exponents of the distributions. Some interesting observations we made using simulations is the formation of clusters, which we identified via image segmentation [54]. The sticking coefficients and the film thickness have dominant effect on the formation of the clusters. At lower sticking coefficients and lower thickness of film, distinct clusters are not formed. At higher sticking coefficients, distinct clusters are formed as the thickness of the film grows.

With the cluster-based model, the degree distribution seems to move more towards power law. In this model as we aggregate the points occupied by a column as a cluster, the degree distribution accrues a thick tail and, more noticeably, a larger sticking coefficient yields a flatter degree distribution, which shows that a cluster-based modeling approach might be better for capturing the shadowing effect. Our clustering approach significantly simplifies

understanding the stochastic shadowing and re-emission effects. The shadowing effect resembles a computer network system, therefore morphology, to form clusters where most of the incident and re-emitted particles start to land on or leave from. Further, the cluster-based model avoids recording the properties and behavior of the particles that are similar because of their physical position on the film. This model rather focuses on the behavior of particles as a group having the same or very similar physical properties. This lays a foundation for our future work where we intend to study the traffic properties of the particles when they travel between various clusters by modeling them as a directed and weighted network and to analyze the growth dynamics of the film.

One of the most important factors in the thin film growth is angle of incidence, which is the angle at which the particles are released on to the film. Different angles result in different growth structure and dynamics on the thin film. We used three different incidences: 0^{o}, 85^{o} and 90^{o}. Another parameter in the simulations was the sticking coefficient, which can play a major role in the shadowing and re-emission effects. In our study, we have used two different sticking coefficients: 0.3 and 0.9. Another property of thin film growth we studied is the film thickness. The thickness is measured in lattice units. One lattice unit is considered to be the thickness of a particle. For this study, we have collected and analyzed data for three different thicknesses: 11, 51, and 101. At these thicknesses, we take a snapshot of the film and these three factors determine a network model [20] to characterize the physical properties of the thin film, e.g., the number, height and width of the hills and valleys formed, and the distances between them.

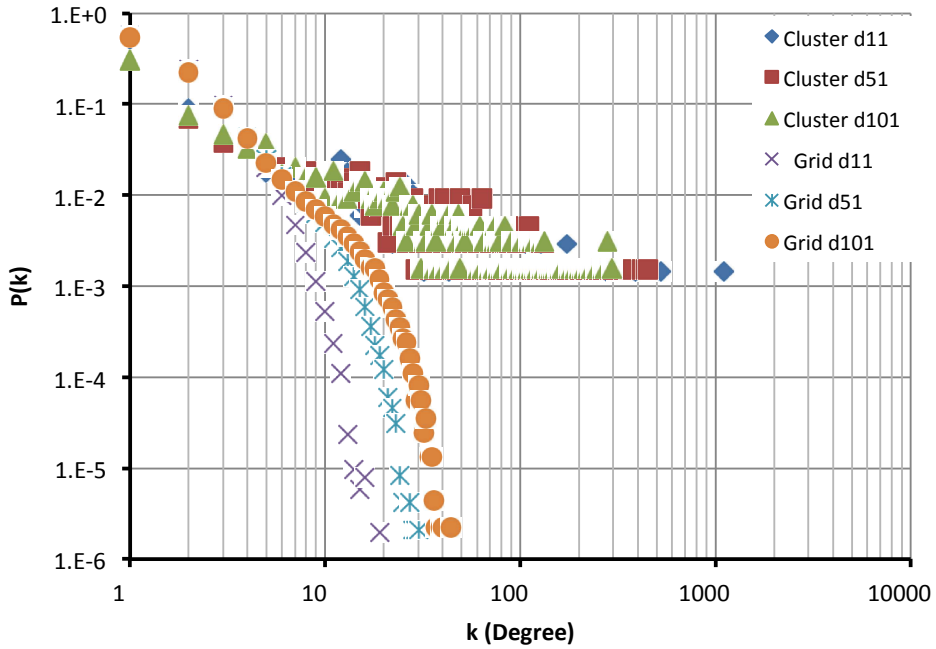

Figure 18: *Cluster and Grid-based model's degree distribution [9]*

Thickness	Grid Based	Cluster Based
d11	-4.664	-0.717
d51	-3.966	-0.728
d101	-3.424	-0.799

Table 2: *Power exponents of Cluster- and Grid-based models [9]*

Two different networks are created using this data, according to cluster-based or grid-based models. In the cluster-based network, each hill and valley is treated as a node of network and the path of particles bouncing between these clusters are treated as links. During the film growth, a snapshot of the film is taken at various thicknesses and the movement of the particles is recorded. A network graph is created using this information and degree distribution is calculated. Following table illustrates power trendline equations for various scenarios discussed above.

	Cluster-based Network	Grid-based Network
Data Series	Equation	Equation
A00_S03_d11	$y = 585.92x^{-2.227}$	$y = 1.7616x^{-5.719}$
A00_S03_d51	$y = 644.43x^{-2.362}$	$y = 1.7072x^{-5.707}$

A00_S03_d101	$y = 862.96x^{-2.616}$	$y = 2.2367x^{-6.022}$
A00_S09_d11	$y = 823.47x^{-2.411}$	$y = 2.1642x^{-5.614}$
A00_S09_d51	$y = 886.27x^{-2.472}$	$y = 2.3031x^{-5.452}$
A00_S09_d101	$y = 788.57x^{-2.24}$	$y = 2.5075x^{-5.483}$
A85_S03_d11	$y = 357.43x^{-2.059}$	$y = 0.0755x^{-1.759}$
A85_S03_d51	$y = 300.41x^{-1.893}$	$y = 0.0892x^{-1.761}$
A85_S03_d101	$y = 357.43x^{-2.059}$	$y = 0.0755x^{-1.759}$
A85_S09_d11	$y = 172.83x^{-1.729}$	$y = 0.0488x^{-1.643}$
A85_S09_d51	$y = 132.74x^{-1.727}$	$y = 0.0313x^{-1.601}$
A85_S09_d101	$y = 101.11x^{-1.945}$	$y = 0.0306x^{-1.626}$
DEP_S03_d11	$y = 1060.6x^{-2.378}$	$y = 0.013x^{-1.915}$
DEP_S03_d51	$y = 1113.8x^{-2.444}$	$y = 0.0134x^{-1.822}$
DEP_S03_d101	$y = 914.53x^{-2.314}$	$y = 0.0133x^{-1.818}$
DEP_S09_d11	$y = 470.63x^{-2.113}$	$y = 1.7933x^{-4.46}$
DEP_S09_d51	$y = 547.22x^{-2.174}$	$y = 0.7607x^{-2.683}$
DEP_S09_d101	$y = 585.92x^{-2.227}$	$y = 0.7201x^{-2.704}$
NODEP_S03_d11	$y = 397.39x^{-2.215}$	$y = 0.0743x^{-1.751}$
NODEP_S03_d51	$y = 344.08x^{-2.062}$	$y = 0.0898x^{-1.766}$
NODEP_S03_d101	$y = 358.76x^{-2.04}$	$y = 0.0743x^{-1.751}$
NODEP_S09_d11	$y = 462.16x^{-2.111}$	$y = 0.0502x^{-1.658}$
NODEP_S09_d51	$y = 592.03x^{-2.235}$	$y = 0.031x^{-1.595}$
NODEP_S09_d101	$y = 603.13x^{-2.166}$	$y = 0.0309x^{-1.631}$

Table 3: *Degree Distribution of Cluster-based and Grid-based Networks*

Each entry under data series pertains to a scenario. For example, A00_S03_d11 represents data set for angle 0^o (A00), sticking coefficient 0.3 (S03) and thickness of 11 (d11). From the table, it can be noticed that the power exponent stays mostly the same (i.e., around -2) in the cluster-based model. Since, the exponent does not change when the factors like sticking coefficient, angle of incidence and thickness of film are changed, the cluster-based model captures a universal behavior in the thin film growth network. But same behavior is not seen between two networks. When the selection criteria for nodes are changed from grid-based to cluster-based, there is a significant change in the exponent, i.e. between -1.5 and -6.0.

		Network Diameter	Graph Density	Modularity	Avg. Clustering Coefficient	Avg. Path Length
Grid Based Model	**So09d11**	2	0.753	0.191	0.753	1.249
	So09d51	2	0.779	0.185	0.544	1.458
	So09d101	2	0.78	0.178	0.782	1.22
	So06d11	2	0.981	0.234	0.981	1.019
	So06d51	2	0.985	0.234	0.984	1.017
	So06d101	2	0.986	0.232	0.884	1.116
	So03d11	2	0.995	0.244	0.993	1.007
	So03d51	2	0.991	0.243	0.991	1.011
	So03d101	2	0.996	0.242	0.994	1.072
Cluster Based Model	**So09d11**	4	0.004	0.486	0.7	2.367
	So09d51	5	0.004	0.489	0.741	2.317
	So09d101	4	0.005	0.485	0.783	2.339
	So06d11	4	0.003	0.481	0.827	2.251
	So06d51	5	0.003	0.463	0.85	2.215
	So06d101	4	0.003	0.482	0.834	2.235
	So03d11	5	0.003	0.456	0.794	2.259
	So03d51	5	0.003	0.468	0.853	2.159
	So03d101	4	0.002	0.427	0.849	2.17

Table 4: *Network Metrics of Cluster-based and Grid-based Networks*

Table 4 illustrates the comparison of some of the network metrics between grid-based and cluster-based networks. As observed from the table, without the loops, the density of the network is very low. This suggests that majority of adatom particle movements are local. Further, the results show that smoothing effect is not prominent between clusters. With the cluster-based network, we can also observe that diameter and average path length of the network are larger, which suggests that particle movements between clusters is reduced – a property of shadowing affect. This shows the cluster-based model is better suited to study the global behavior of thin film growth and shadowing phenomenon.

Another interesting phenomenon we studied is the small world phenomenon. We have used number of nodes and edges from networks formed at various thickness of substrate and

calculated average length and clustering coefficient. We then used same nodes and edges and built a random network using Gephi tool. We then calculated average length of the network and clustering coefficient.

			Thin Film N/W	Random N/W	Thin Film N/W	Random N/W
	Nodes	Edges	Clustering Coefficient	Clustering Coefficient	Path length	Path length
Height d-1	665	2115	0.690	0.051	2.373	2.126
Height d-11	683	2799	0.699	0.050	2.355	2.129
Height d-21	666	3000	0.693	0.049	2.370	2.118
Height d-41	658	3471	0.686	0.050	2.310	2.142
Height d-51	661	3572	0.684	0.050	2.318	2.137
Height d-61	661	3667	0.674	0.050	2.330	2.137
Height d-71	667	3687	0.692	0.050	2.311	2.129
Height d-91	658	3725	0.688	0.051	2.351	2.142
Height d-101	663	3877	0.670	0.050	2.311	2.134
Height d-121	652	3896	0.665	0.050	2.310	2.143
Height d-131	641	3918	0.654	0.048	2.291	2.148
Height d-141	644	3815	0.671	0.049	2.323	2.147

Table 5: Path length and clustering coefficients for thin film network and corresponding E-R random graph.

Table 5 shows the comparisons of these statistics for various thin film networks and corresponding random networks. It can be observed from the table that the path lengths and clustering coefficients of thin film networks are greater than the E-R random graphs. Thus, we can conclude that thin film networks demonstrate small world characteristics.

Chapter 5: Traffic Modeling for Thin-Film Growth

As described in the earlier chapters, applying network theory to thin film growth helped us understand the growth dynamics of thin film growth. Similarly, we will apply the traffic models and traffic statistics to the growth phenomenon and study the characteristics of interaction between the adatoms when they land on different points of the substrate and bounce around some more points before settling down. As the thin film grows and the hills are formed, we expect them to act as initial landing spots before the particle bounces off and settles on a point. This movement of the adatoms can be treated as flow of packets in the network traffic. Studying the particle movement in thin film growth can give us statistics like inter-arrival time of the particles, and help us find out if there are certain points on the substrate that act as hubs and attract more particles.

In a typical traffic model of a network, one counts the number of arrivals at a link or node. This counting process produces a time series of the traffic, which then can be used to analyze various statistics of the network traffic. This time series study could give us some insights in how sticking coefficient and thickness of film will influence the shadowing and smoothing effects on the thin film growth. In order to develop an understanding of time in the film growth process, we use a fixed number of particles flowing into gas chamber as equivalent to a time unit and develop the traffic time series based on that time unit. In this model, we would simulate over a billion particles flowing through the chamber and map the traffic flow for various time units. For example, we would study the inter-arrival time of particles using the thickness of the thin-film as the unit of time and develop the traffic counting process as a time series based on that model. As the thickness grows by one lattice unit we will consider this as a time unit and study the traffic statistics.

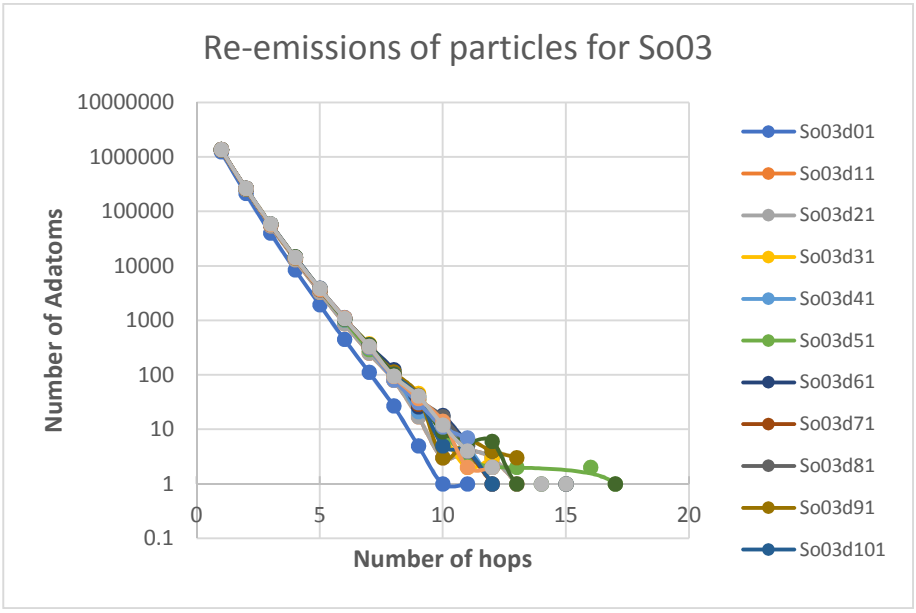

(a)

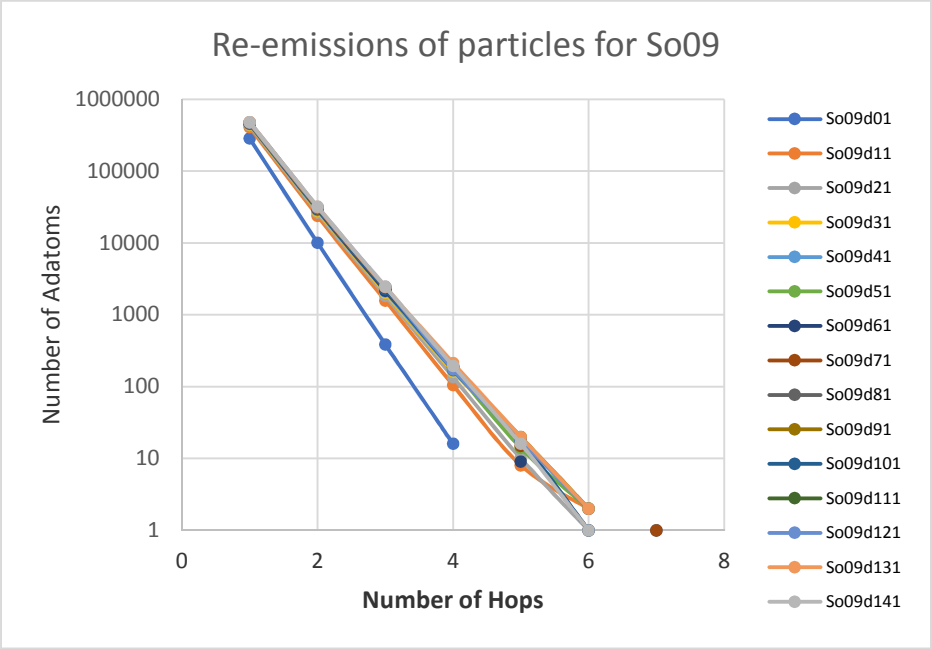

(b)

Figure 19: Number of re-emissions of particles at different thickness for sticking coefficients So=0.3 and 0.9

Figure 19 shows the number of re-emissions every particle goes through after initial contact with the substrate. At lower sticking coefficients (0.3), the number of particles bouncing multiple times after the initial contact is greater when compared to the process with higher

sticking coefficients. By bouncing multiple times, the particles cause the smoothing effect. Hence it can be concluded that at lower sticking coefficients smoothing effect is more predominant, which is an expected outcome. Figure 20 is a rescaled range (R/s) statistic plot to determine the Hurst exponent. For a given sample size n, R/s statistic is defined as following [108]:

$$\frac{R}{s} = \frac{1}{s}\{max_k\left(\sum_1^k (x_i - \bar{x})\right) - min_k\left(\sum_1^k (x_i - \bar{x})\right)\} \qquad (11)$$

where $1 \leq k \leq n$, $\bar{x} = \sum x / n$ and $s^2 = \sum (x - \bar{x})^2 / n$, with the summations taken 1 to n. From the plot, it can be noted that the Hurst exponent is between 0.530 and 0.825. We have also plotted an autocorrelation function (ACF) of the traffic time series for sticking coefficient 0.9 as seen in Figure 21. It can be noted from the plot that the ACF does not display any correlation between traffic for this simulation set. We will further investigate ACF for different sticking coefficients and different time units.

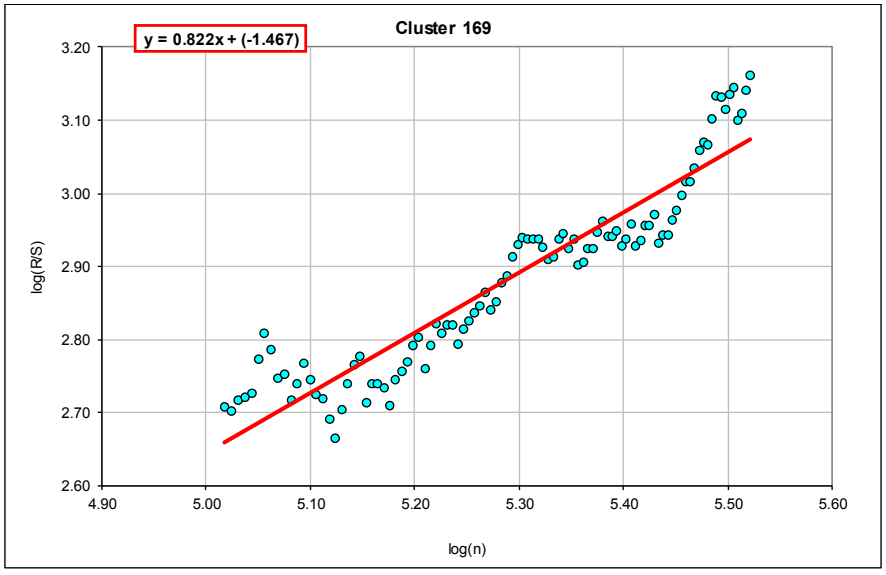

(a)

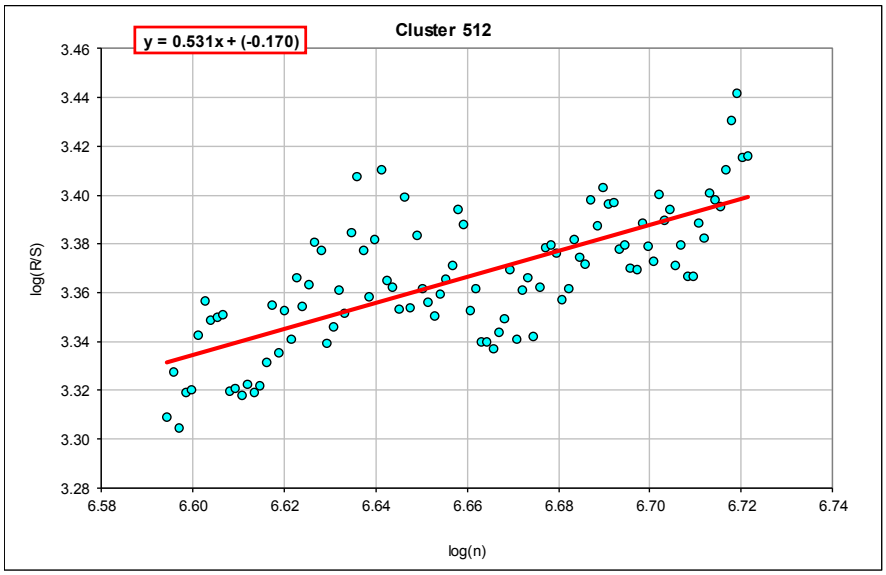
Cluster 512
y = 0.531x + (-0.170)
log(R/S)
log(n)
3.46
3.44
3.42
3.40
3.38
3.36
3.34
3.32
3.30
3.28
6.58
6.60
6.62
6.64
6.66
6.68
6.70
6.72
6.74

(b)

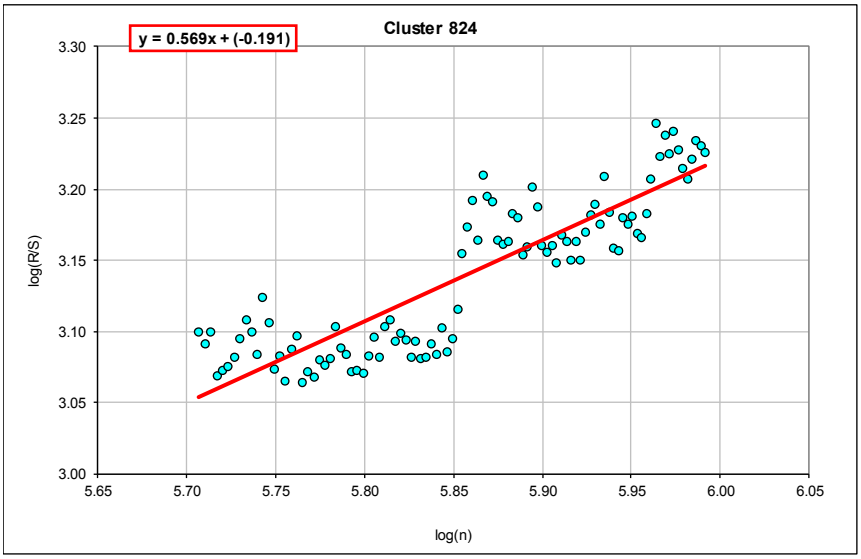
Cluster 824
y = 0.569x + (-0.191)
log(R/S)
log(n)
3.30
3.25
3.20
3.15
3.10
3.05
3.00
5.65
5.70
5.75
5.80
5.85
5.90
5.95
6.00
6.05

(c)

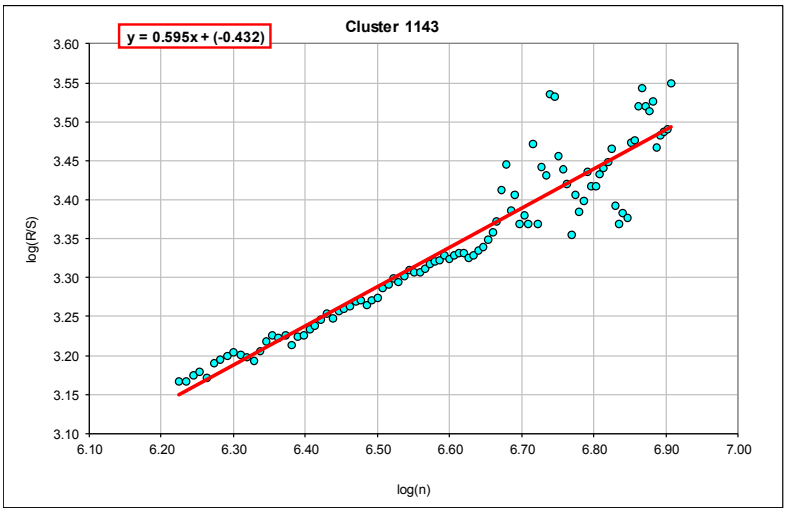

(d)

Figure 20: Hurst exponent *for traffic on various cluster formed on substrate with sticking coefficient 0.9*

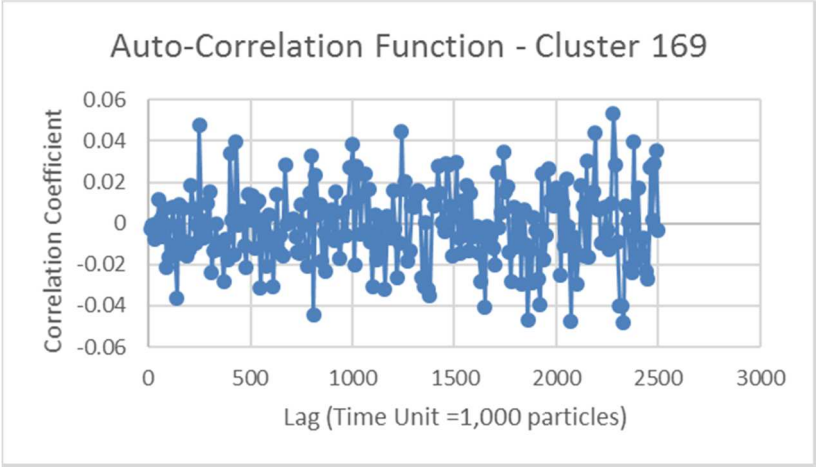

(a)

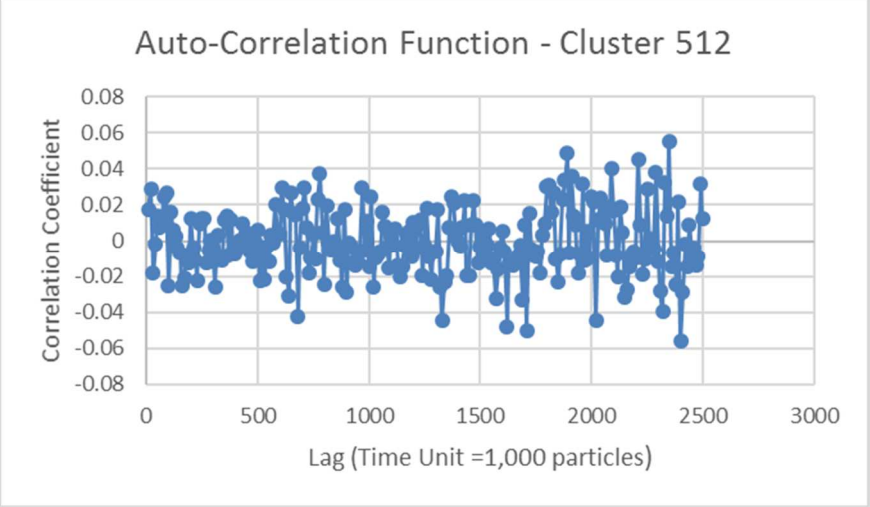

(b)

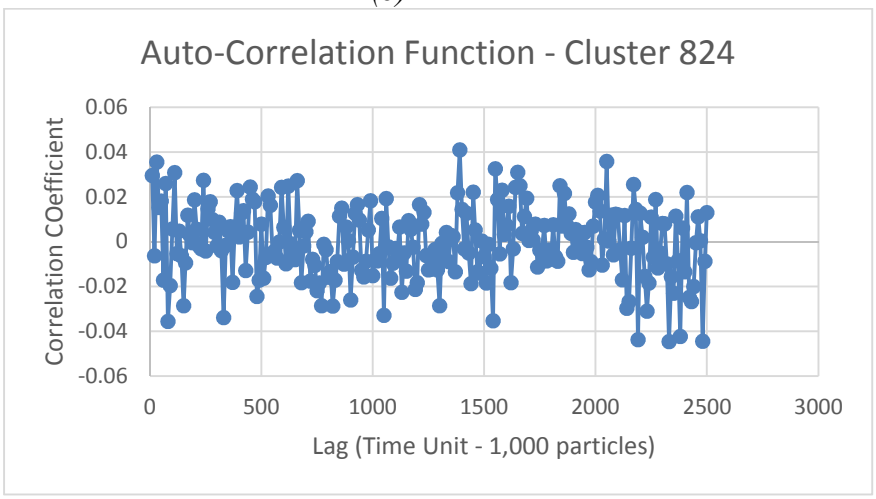

(c)

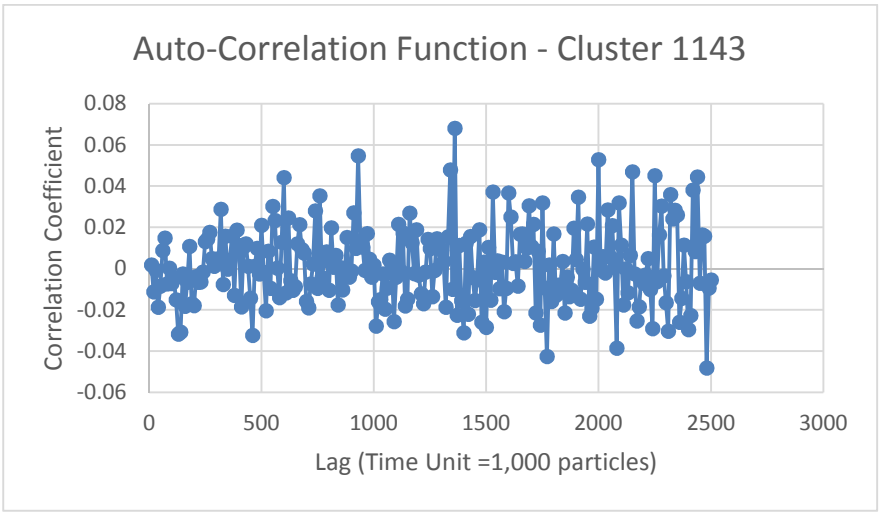

(d)

Figure 21: *Autocorrelation Function for traffic on various cluster formed on substrate with sticking coefficient 0.9*

Figure 22 shows the particle traffic as time series at various clusters over a period. We have considered 1000 particles released into gas chamber as one unit of time and plotted number of particles arriving at different clusters. As expected, the traffic is not uniformly distributed among the clusters and we observe existence of hubs or power centers on the substrate.

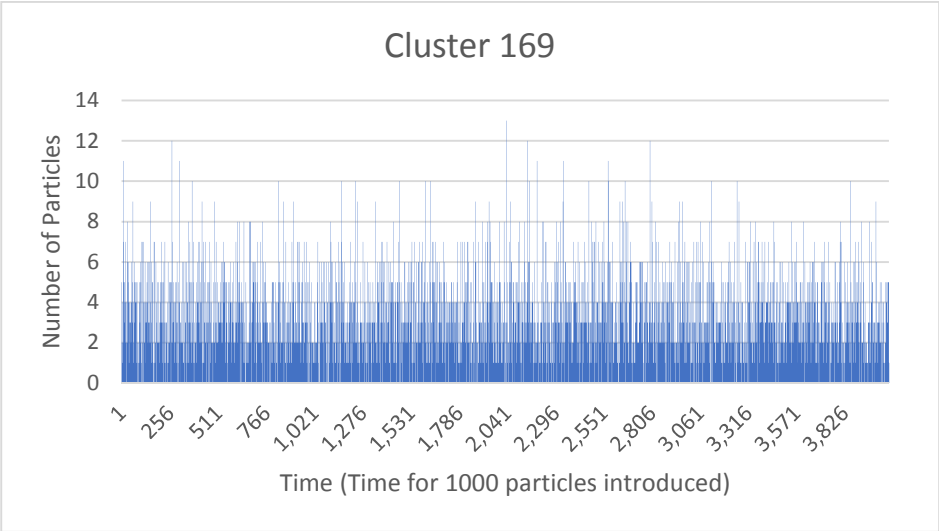

(a) Average traffic rate is 2.55 particles per 1,000 new particles

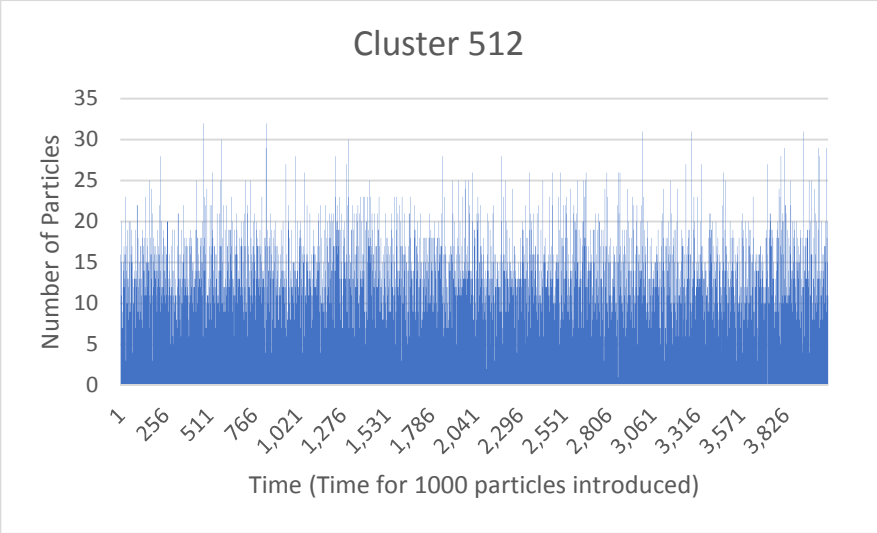

(b) Average traffic rate is 11.89 particles per 1,000 new particles

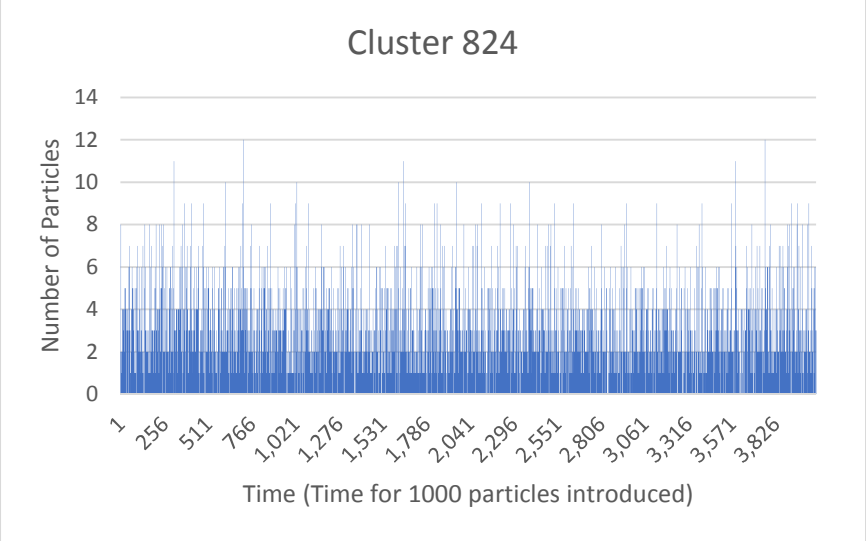

(c) *Average traffic rate is 2.35 particles per 1,000 new particles*

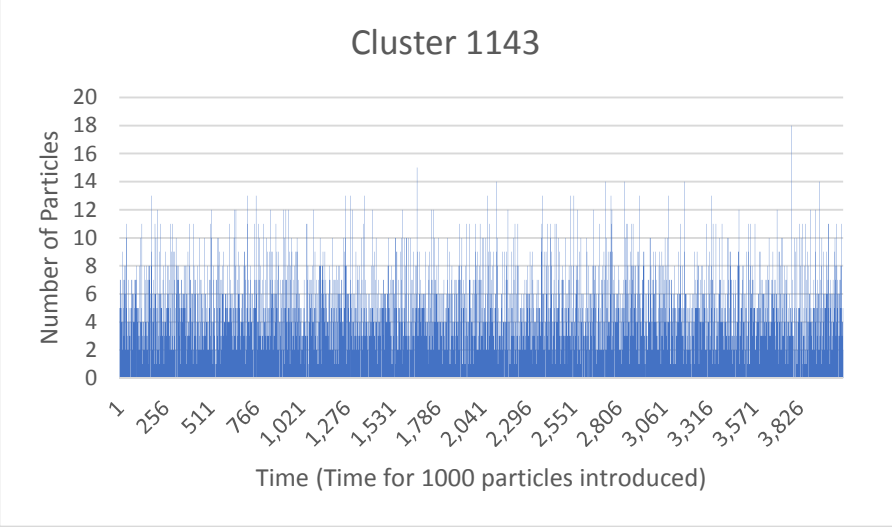

(d) Average traffic rate is 4.19 particles per 1,000 new particles

Figure 22: Traffic on different clusters

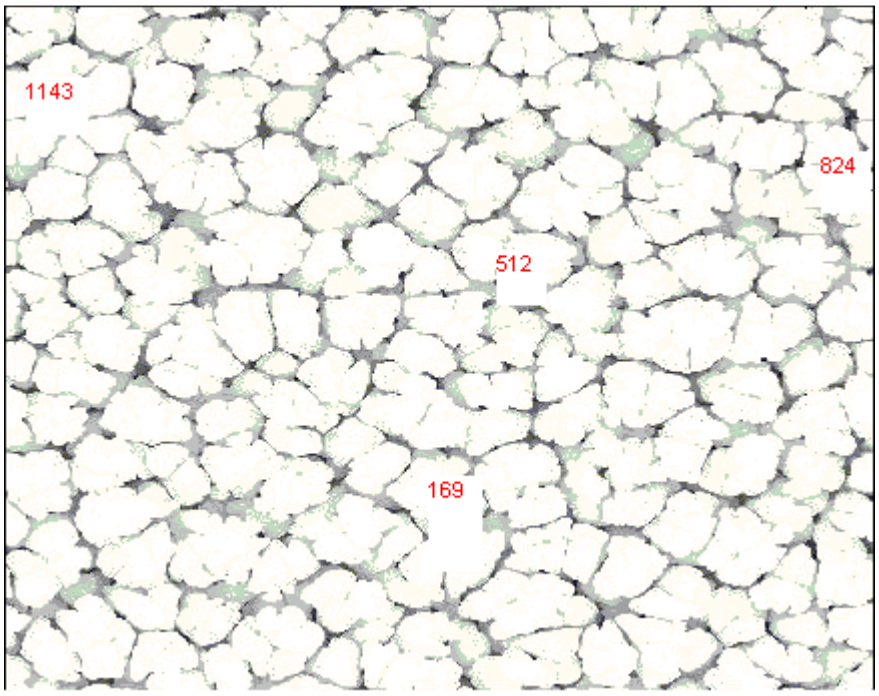

Figure 23*: *The clusters studied for traffic model on the substrate

We chose clusters based on their physical location on the substrate. And we have modeled the traffic flow on these clusters. As can be noted from the plots, there is a clear variation of traffic on different clusters. One more interesting observation we made is the clusters that are located near the edges of the substrate attract low traffic compared to the clusters that are located at inner parts of the substrate. In the Figure 22, cluster 512 is located near the center of the substrate, whereas cluster 824 and cluster 1143 are located near edges. Cluster 169 is located away from edges and the center of the substrate. This is an important observation as it provides the physical area at which the probability of hub formation on the substrate is high. By controlling these areas by adjusting various factors like thickness and sticking coefficients, the smoothness of the substrate can be managed.

Chapter 6: Conclusions and Future Work

6.1 Conclusions

Often in thin film growth, we observe that important statistical surface parameters show "power law" scaling with time. For example, root-mean-square roughness (i.e. root-mean-square height fluctuations), lateral correlation length (i.e. average hill size), and surface wavelength (i.e. average peak-to-peak separation of hills) all dynamically change with growth time having a specific power exponent (~tp). The values of these exponents depend on the dominant growth mechanisms (e.g. shadowing, value of sticking coefficient, surface diffusion, and noise). These surface parameters and their exponents also affect the trajectories and therefore dynamic network topology of the re-emitted particles. For example, in the case of columnar growth where shadowing effect is dominant and sticking coefficients are large, peak-to-peak separation (wavelength) of hills will be increasing with growth time according to a power law relation (~tp). In such a growth system, peak-to-peak separation can be thought as similar to node-to-node separation in a network system. So, in this specific growth case, one might expect that nodes will be coming further apart with time obeying a power law relation. This also means that some nodes (hills) can become stronger (e.g. higher height) while some others can get weaker (e.g. get shadowed). Therefore, amount of traffic per node (e.g. surviving hill) can also be increasing according to a power law or another well-described analytical relation. In addition, during columnar growth, re-emitted particles will mainly be bouncing off from the peaks of hills and get deposited to other neighboring hill tops, as observed in our initial Monte Carlo simulation results. Consequently, average network link lengths (i.e. propagation delays on links) will also be expected to dynamically change obeying a heavy-tail distribution with a tail (or a power law distribution with an exponent) value similar to that of peak-to-peak separation.

Interestingly, some "ad hoc" networks exhibit a similar behavior. Functions of nodes can change in ad hoc network with a lot of dynamism in them. For example, a mobile ad hoc network of several nodes can yield some nodes to become cluster heads due to the optimality of selecting those nodes as cluster heads. Later on in time, these cluster heads might become regular nodes because their position is not best suited to stay as cluster heads. Such behavior cannot be observed in "fixed" (or close to fixed) networks where nodes and links do not change a lot. But, networks with lots of mobile nodes in them can exhibit such behavior. Potential similarities (especially in topology changes and traffic changes) between the growth and other well-known real networked systems (e.g. communication or traffic networks) in terms of such dynamic characteristics would be an additional benefit/result of our study.

While the grid-based model captures different properties in the way nodes are identified, the cluster-based model hides some of the local interactions within the lattice points in a cluster. Thus, the cluster-based model will help researchers identify global behavior of thin film and avoid any noise that might be originating due to local interactions. This comparison of degree distribution between two networks sheds light on various factors that would impact the characteristics of thin film growth phenomenon. We also analyze the community structure in the network. Communities are groups of nodes and their edges that share common properties (e.g., being on the same column) or influence the network in a similar way [10]. For example, in World Wide Web some pages exist that deal with a common typic that are related to each other by the subject they are dealing with. Community detection is important for other reasons, too. Identifying communities is very important because it allows classification of nodes, according to their topological positions.

Typically, the nodes are very well connected inside a community whereas the nodes in different communities are sparsely connected. Community detection also allows us to obtain a coarse-grained description of the original network. In this paper, we believe the finding of communities in our film growth network reveals a better understanding of the columnar structures. Our future aim is to model thin film growth as a network system and try to understand its statistics and dynamics by means of such a network-based model.

6.2 Future Work

6.2.1 Dynamic Network Behavior

The quantitative results of dynamic network behavior will lead to a detailed understanding of dynamic network phenomena during the growth process of various kinds of thin film deposition systems and aims to reveal universal growth behavior properties. Using the Monte Carlo simulation and grid network model approaches explained above, we will investigate various dynamic network behaviors, including, but not limited to:

(i) Routing of atoms (e.g., do all atoms go to their final destination by means of the shortest path or are other factors involved?) from their initial point of falling on the film to their final point of settlement on the film,

(ii) Dynamical change in the morphology-dependent network behavior due to the dynamic evolution of surface topography, shadowing locations, and re-emission paths as briefly discussed in the previous sections, and

(iii) Effects of sticking coefficient (i.e. re-emission), oblique angle (shadowing), surface diffusion, and initial surface topography on the dynamic networking behavior during growth.

6.2.2 Development of Analytical/Empirical Network Models

We will analyze the community structure in the network. In this project, we believe the finding communities in our film growth network will reveal a better understanding of the columnar structures by using the latest community structure algorithms. However, we note that our main objective in this proposal is not to explain thin film growth with real networked systems or vice versa. Our aim is to model thin film growth as a network system and try to understand its statistics and dynamics by means of such a network-based model.

References

[1]. K. Borner, S. Sanyal, A. Vespignani, Network Science, Indiana University, Annual Review of Information Science & Technology; 2007

[2]. O. Mason and M. Verwoerd, Graph Theory and Networks in Biology. IET Systems Biology, 1:89 – 119.

[3]. J. A. Dunne, R. J. Williams, and N. D. Martinez (2002), Network structure and biodiversity loss in food webs: robustness increases with connectance. Ecology Letters, 5: 558–567. doi:10.1046/j.1461-0248.2002.00354.x

[4]. J. E. Cohen, F. Briand, and C. M. Newman, Community Food Webs: Data and Theory, Springer-Verlag, New York, 1990.

[5]. R. Guimera, L. Danon, A.Diaz-Guilera, F.Giralt, A.Arenas, Self-similar community structure in a network of human interactions. Physical Review. E, Statistical, nonlinear, and soft matter physics, 12/2003, Volume 68, Issue 6 Pt 2

[6]. J. H. Fowler and N.A. Christakis, Cooperative behavior cascades in human social networks. PNAS 2010 107 (12) 5334-5338

[7]. R. Milo, S. Shen-Orr, S. Itzkovitz, N. Kashtan, D. Chklovskii, U. Alon, Network Motifs: Simple building blocks of complex networks, Science October 2002, Vol. 298 no. 5594 pp. 824-827

[8]. R. Albert and A.L. Barabasi, Statistical mechanics of complex networks, Rev. Mod. Phys. 74, 47 (2002).

[9]. S. N. Dorogovtsev and J. F. F. Mendes, Evolution of networks, Adv. Phys. 51, 1079 (2002).

[10]. M. E. J. Newman, The structure and function of complex networks, SIAM Review 45, 167 (2002).

[11]. M. E. J. M. E. J. Newman, S. H. Strogatz, and D. J. Watts, Random graphs with arbitrary degree distributions and their applications, *Phys. Rev. E* 64, 026118 (2001)

[12]. M. E. J. Newman, Networks: An Introduction, Oxford University Press, Inc., New York, NY, 2010, pages 35-38.

[13]. L. da F. Costa, F. A. Rodrigues, G. Travieso & P. R. Villas Boas, Characterization of complex networks: A survey of measurements, Advances in Physics, Volume 56, Issue 1, 2007

[14]. A.L. Barabasi, Network Science book, pages 10-15, 26,27. November, 2014 Retrieved from http://barabasilab.neu.edu/networksciencebook

[15]. J. Leskovec, J. M. Kleinberg, and C. Faloutsos. Graphs over time: densification laws, shrinking diameters and possible explanations, In KDD '05, 2005.

[16]. R. Kumar, P. Raghavan, S. Rajagopalan, D. Sivakumar, A. Tomkins, and E. Upfal. Stochastic models for the web graph, In FOCS '00, page 57, 2000.

[17]. E.M. Airoldi, D. M. Blei, S.E. Fienberg, and E.P. Xing, Mixed membership stochastic block models. JMLR, 9:1981-2014, 2007.

[18]. M. Kim, and J. Leskovec, Modeling Social Networks with Node Attributes using the Multiplicative Attribute Graph Model, Proceedings of Conference on Uncertainty in Artificial Intelligence, 2011

[19]. A. Goldenberg, A.X. Zheng, S.E. Fienberg, E.M. Airoldi. A Survey of Statistical Network Models. Foundations and Trends in Machine Learning, 2(2):1-117, 2009.

[20]. D. Ni and P. D. Christofides. Dynamics and control of thin film surface microstructure in a complex deposition process. (2005) Chemical Engineering Science, 60 (6), pp. 1603-1617.
[21]. M. Yuksel, T. Karabacak and H. Guclu. Network behavior in thin film and nanostructure growth dynamics. Proceedings of the 2nd international conference on Nano-Networks, Catania, Italy, 2007.
[22]. D. L. Smith, Thin-Film Deposition: Principles and Practice (McGraw-Hill, New York, 1995.
[23]. P. Meakin, Fractals, Scaling, and Growth Far from Equilibrium. Cambridge University Press, Cambridge, England, 1998. Pages 46-48
[24]. A.-L. Barabasi and H. E. Stanley, Fractal Concepts in Surface Growth. Cambridge University, Cambridge, England, 1995.
[25]. N. O. Young and J. Kowal, Optically active fluorite films, Nature 183, 104 (1959).
[26]. T. Motohiro and Y. Taga, Thin film retardation plate by oblique deposition, Appl. Opt. 28, 2466 (1989).
[27]. R. M. Azzam, Chiral thin solid films: Method of deposition and applications, Appl. Phys. Lett. 61, 3118 (1992).
[28]. K. Robbie, M. J. Brett, and A. Lakhtakia, Chiral sculptured thin films, Nature 384, 616 (1996).
[29]. K. Robbie, G. Beydaghyan, T. Brown, C. Dean, J. Adams, and C. Buzea, Ultrahigh vacuum glancing angle deposition system for thin films with controlled three-dimensional nanoscale structure, Rev. Sci. Instrum. 75, 1089 (2004).
[30]. T. Karabacak and T.-M. Lu, Chapter: Shadowing growth and physical self-assembly of 3D columnar structures, in Handbook of Theoretical and Computational Nanotechnology, edited by M. Rieth and W. Schommers (American. Scientific Publishers, Stevenson Ranch, CA, 2005), chap. 69, p. 729.
[31]. T. Karabacak, G.-C. Wang, and T.-M. Lu, Physical self-assembly and the nucleation of 3D nanostructures by oblique angle deposition, J. Vac. Sci. Technol. A 22, 1778 (2004).
[32]. A. Lakhtakia and R. Messier, Sculptured Thin Films: Nanoengineered Morphology and Optics (SPIE Press, Bellingham, WA, 2005).
[33]. S.N. Dorogovtsev and J.F.F. Mendes, Evolution of Networks, From Biological Nets to the Internet and WWW. Oxford University Press March, 2003.
[34]. F. Family and T. Vicsek, Scaling of the active zone in the Eden process on percolation networks and the ballistic deposition model, J. Phys. A 18, L75 (1985).
[35]. F. Family, Scaling of rough surfaces: effects of surface diffusion, J. Phys. A 19, L441 (1986).
[36]. R.P.U. Karunasiri, R. Bruinsma, and J. Rudnick, Thin-film growth and the shadow instability. Phys. Rev. Lett. 62, 788 (1989).
[37]. T.-M. Lu, Y.-P. Zhao, J.T. Drotar, T. Karabacak, and G.-C. Wang, Novel mechanisms of the growth morphology thin films, Mat. Res. Soc. Symp. Proc. 749, 3 (2003).
[38]. M. Pelliccione, T. Karabacak, and T.-M. Lu, Breakdown of dynamic scaling in surface growth under shadowing, Phys. Rev. Lett. 96, 146105 (2006).
[39]. M. Pelliccione, T. Karabacak, C. Gaire, G.-C. Wang, and T.-M. Lu, Mound formation in surface growth under shadowing, Phys. Rev. B 74, 125420 (2006).
[40]. T. Karabacak, Y.P. Zhao, G.C. Wang, T.M. Lu, Growth front roughening in silicon nitride films by PECVD, Phys. Rev. B 66, 075329 (2002).
[41]. X. Xu and D. W. Goodman, Metal deposition onto oxides: An unusual low initial sticking probability for copper on $Si0_2$, Appl. Phys. Lett. 61, 1799 (1992).

[42]. D. Easley and J. Kleinberg, Networks, Crowds, and Markets: Reasoning About a Highly Connected World. Cambridge University Press, 2010. Pages 23-28
[43]. P. Meakin, Fractals, Scaling, and Growth Far from Equilibrium. Cambridge University Press, Cambridge, England, 1998.
[44]. T. Karabacak, J.P. Singh, Y.P. Zhao, G.C. Wang, and T.M. Lu, Scaling during shadowing growth of isolated nano-columns, Phys. Rev. B 68, 125408 (2003).
[45]. T. Karabacak, G.-C. Wang, and T.-M. Lu, Quasi-periodic nano-structures grown by oblique angle deposition, J. Appl. Phys. 94, 7723 (2003).
[46]. T. Smy, D. Vick, M. J. Brett, S. K. Dew, A. T. Wu, J. C. Sit, and K. D. Harris, Three-dimensional simulation of film microstructure produced by glancing angle deposition, J. Vac. Sci. Technol. A 18, 2507 (2005).
[47]. J.T. Drotar, Y.P. Zhao, T.M. Lu, and G.C. Wang, Why is KPZ type surface roughening so hard to observe?, Mat. Res. Soc. Symp. Proc. 648, P7.9.1 (2001).
[48]. T. Karabacak and T.-M. Lu. Handbook of Theoretical and Computational Nanotechnology, chapter Shadowing growth and physical self-assembly of 3D columnar structures, page 729. American Scientific Publishers, Stevenson Ranch, CA, 2005.
[49]. Y.-P. Zhao, G.C. Wang, and T.-M. Lu, Characterization of Amorphous and Crystalline Rough Surfaces: Principles and Applications. Academic Press, 2001.
[50]. D. Kondor, M. Pósfai, I. Csabai, G. Vattay. Do the Rich Get Richer? An Empirical Analysis of the Bitcoin Transaction Network *PLoS ONE*, Vol. 9, No. 2. (5 February 2014)
[51]. S. N. Dorogovtsev and J. F. F. Mendes, Evolution of Networks: From Biological Nets to the Internet and WWW, Oxford University Press, Oxford, 2003.
[52]. R. Albert, H. Jeong, and A.L. Barabasi, Internet: Diameter of the World-Wide Web, Nature 401, 130 (1999).
[53]. U. Stelzl, U. Worm, M. Lalowski , Haenig C, Brembeck FH, Goehler H, Stroedicke M, Zenkner M, Schoenherr A, Koeppen S, Timm J, Mintzlaff S, Abraham C, Bock N, Kietzmann S, Goedde A, Toksöz E, Droege A, Krobitsch S, Korn B, Birchmeier W, Lehrach H, Wanker EE, A human protein-protein interaction network: a resource for annotating the proteome, Cell. 2005 Sep 23;122(6):957-68
[54]. T. Karabacak, H. Guclu, and M. Yuksel, Network Behavior in Thin Film Growth Dynamics, Physical Review B, Volume 79, Issue 19, May 2009.
[55]. S. Badepalli, M. Yuksel, T. Karabacak, and H. Guclu. Network Analysis of Clusters to Capture Shadowing and Re-emission Effects in Thin Film Growth, NetSci 2013, June 2013.
[56]. R.W. Berry, P.M. Hall, M.T. Harris, Thin Film Technology. Van Nostrand Reinhold, Princeton, NJ 1967. Pages 28 - 35.
[57]. M.B. Small, and D.J. Pearson, On-Chip Wiring for VLSI: Status and Directions, IBM J. Res. Dev., 34(6):858 (1990)
[58]. J.R. Black, Electromigration-A Brief Survey and Some Recent Results, IEEE Trans. Electron. Dev., 16:338 (1969)
[59]. J.R. Lloyd, and P.M. Smith, Electromigration Lifetime of Al/Cu Thin Film Conductors, J. Vac. Sci. Technol., 1(12):455 (1983)
[60]. P.M. Solomon, The Need for Low Resistance Interconnections in Future High Speed Systems, SPIE, 947:104 (1988)
[61]. O. Milton, Materials Science of Thin Films, Second Edition: Deposition and Techniques. October 2001. Academic Press. Pages 64 - 67.

[62]. Rointan Framroze Bunshah, Handbook of deposition technologies for films and coatings: science, technology, and applications. Elsevier, November 2009. Pages 5-10.
[63]. D.L. Smith, Thin-film deposition: principles and practice. McGraw-Hill Professional; 1 edition March, 1995. Pages 57.
[64]. M.L. Hitchman , K.F. Jensen, Chemical Vapor Deposition Principles and Applications. Academic Press; 1 edition April, 1993. Pages 33.
[65]. E. M. van Veldhuizen and F. J. de Hoog, Analysis of a Cu-Ne hollow cathode glow discharge at intermediate currents, J. Phys. D: Appl. Phys. 17, 953 (1984).
[66]. A. Bogaerts, J. Naylor, M. Hatcher, W. J. Jones, and R. Mason, Influence of sticking coefficients on the behavior of sputtered atoms in an argon glow discharge: Modeling and comparison with experiment, J. Vac. Sci. Technol. A 16, 2400 (1998).
[67]. K. Obara, Z. Fu, M. Arima, T. Yamada, T. Fujikawa, N. Imamura, and N. Terada, Collision processes between sputtered particles on high speed rotating substrate and atomic mass dependence of sticking coefficient, J. of Crystal Growth 237–239, 2041 (2002).
[68]. S. Migita, K. Sakai, H. Ota, Z. Mori, and R. Aoki, The influence of Bi-sticking coefficient in the growth of Bi(2212) thin film by ion beam sputtering, Thin Solid Films 281-282, 510 (1996).
[69]. A. Bogaerts, E. Wagner, B. W. Smith, J. D. Winefordner, D. Pollmann, W. W. Harrison, and R. Gijbels, Three-dimensional density profiles of sputtered atoms and ions in a direct current glow discharge: experimental study and comparison with calculations, Spectrochimica Acta Part B 52, 205 (1997).
[70]. A. J. Toprac, B. P. Jones, J. Schlueter, and T. S. Cale, Modeling of collimated titanium nitride physical vapor deposition using a combined specular-diffuse formulation, Mat. Res. Soc. Symp. Proc. 355, 575 (1995).
[71]. O. Yamazaki, K. Iyanagi, S. Takagi, and K. Nanbu, Modeling of Cu transport in sputtering using a Monte Carlo simulation, Jpn. J. Appl. Phys. 41, 1230 (2002).
[72]. D. Liu, S. K. Dew, M. J. Brett, T. Smy, and W. Tsai, Compositional variations in Ti-W films sputtered over topographical features, J. Appl. Phys. 75, 8114 (1994).
[73]. R. J. Buss, P. Ho, W. G. Breiland, and M. E. Coltrin, Reactive sticking coefficients of silane on silicon, in Deposition and Growth: Limits for Microelectronics, edited by G. W. Rubloff, AIP Conf. Proc. 167, 34 (1988).
[74]. J.A. Norrell, Network Dynamics and Systems Biology. 2011, ProQuest UMI. Page 2.
[75]. C.P. Christensen, Inference, Simulation, Modeling, and Analysis of Complex Networks in Systems Biology, 2007, ProQuest UMI page 16.
[76]. R. Diestel Graph theory. Springer; 4th edition. 2010. Pages 122.
[77]. V. Latora and M. Marchiori. Efficient behavior of small-world networks. Physics Review Letters, 87:198701, 2001
[78]. R. Monasson. Diffusion, localization and dispersion relations on small-world lattices. European Physical Journal B, 12(555), 1999.
[79]. M. E. J. Newman and D. J. Watts. Renormalization group analysis of the small-world network model. Physical Review Letters A , 263:341–346, 1999.
[80]. C. Teuscher, Nature-inspired interconnects for self-assembled large-scale network-on-chip designs, Chaos 17, 026106 (2007).
[81]. A.-L. Barabási, R. Albert, and H. Jeong. Scale-free characteristics of random networks the topology of the world wide web. Physica A, 281:69–77, 2000.
[82]. A.-L. Barabási and E. Bonabeau. Scale-free networks. Scientific American ,288:60–

69, 200.
[83]. world network model. Physical Review Letters A , 263:341–346, 1999.
[84]. M. Girvan and M. E. J. Newman. Community structure in social and biological networks. Proceedings of the National Academy of Science USA,99(12):7821–7826, 2002.
[85]. R. Guimerà, S. Mossa, A. Turtschi, and L. A. N. Amaral. The worldwide air transportation network: Anomalous centrality, community structure, and cities' global roles. Proceedings of the National Academy of Science USA,102:7794–7799, 2005.
[86]. V. Gol'dshtein, G. A. Koganov, and G. I. Surdutovich. Vulnerability and hierarchy of complex networks. cond-mat/0409298, 2004.
[87]. J. T. Drotar, Y.-P. Zhao, T.-M. Lu, and G.-C. Wang, Mechanisms for plasma and reactive ion etch-front roughening, Phys. Rev. B 61, 3012 (2000).
[88]. Simon, H. A., On a class of skew distribution functions, Biometrika 42, 425–440 (1955).
[89]. M. Kochen, Ed., The Small-World. Norwood: Ablex, 1989.
[90]. P. Dodds, R. Muhamad, and D. Watts, An experimental study of search in global social networks, Science, vol. 301, pp. 827-9, 2003.
[91]. Mark D. Humphries, Kevin Gurney, Network 'Small-World-Ness': A Quantitative Method for Determining Canonical Network Equivalence, PLoS ONE, Edited by Olaf Sporns, vol. 3, issue 4, p. e0002051
[92]. Hao Jiang - Constantinos Dovrolis, Why is the internet traffic bursty in short time scales?, ACM SIGMETRICS Performance Evaluation Review – 2005
[93]. Victor S. Frost and Benjamin Melamed, "Traffic Modeling for Telecommunications Networks", IEEE Communications, Mar. 1994
[94]. Hossien bidgoli, The handbook of computer Networks, - Wiley Publishing ©2007
[95]. Li, Ting. "Background Traffic Modeling for Large-Scale Network Simulation." (2014).
[96]. R. Cohen and S. Havlin, Scale-free networks are ultra-small, Phys. Rev. Lett. 90, 058701 (2003).
[97]. W. E. Leland, M. S. Taqqu, W. Willinger, and D. V. Wilson, On the self-similar nature of Ethernet traffic (extended version), IEEE/ACM Transactions on Networking 2, 1 (1994).
[98]. M. E. Crovella and A. Bestavros,Self-similarity in World Wide Web traffic: evidence and possible causes, IEEE/ACM Transactions on Networking 5, 835 (1997).
[99]. S. Fortunato, C. Castellano, Community structure in graphs, in Springer's Encyclopedia of Complexity and System Science (2008).
[100]. Will E. Leland, Murad S. Taqqu, Walter Willinger, and Daniel V. Wilson. On the self-similar nature of Ethernet traffic (extended version). IEEE/ACM Transactions on Networking, 2(1):1–15, 1994.
[101]. Chandrasekaran, Balakrishnan. Survey of network traffic models. Waschington University in St. Louis CSE 567 (2009).
[102]. Fraleigh, Chuck, et al. "Packet-level traffic measurements from the Sprint IP backbone." IEEE network 17.6 (2003): 6-16.
[103]. Crovella, Mark E., and Azer Bestavros. "Self-similarity in World Wide Web traffic: evidence and possible causes." IEEE/ACM Transactions on networking 5.6 (1997): 835-846.

[104]. J Tang, Y Wang, H Wang, S Zhang, F Liu, Dynamic analysis of traffic time series at different temporal scales: A complex networks approach, Physica A: Statistical Mechanics and its Applications 405, 303-315

[105]. D. Easley and J. Kleinberg, Networks, Crowds, and Markets: Reasoning About a Highly Connected World. Cambridge University Press, 2010. Pages 23-28.

[106]. UTHSCSA Image Tool, http://compdent.uthscsa.edu/dig/itdesc.html

[107]. Dunne, J. A. , Williams, R. J. and Martinez, N. D. (2002), Network structure and biodiversity loss in food webs: robustness increases with connectance. Ecology Letters, 5: 558–567. doi:10.1046/j.1461-0248.2002.00354.x

[108]. D. Conniffe & J. E. Spencer, Approximating the Distribution of the R/s Statistic, The Economic and Social Review, Economic and Social Studies, 2000, vol. 31(3), pages 237-248.

[109]. S. Fortunato, C. Castellano, Community structure in graphs, in Springer's Encyclopedia of Complexity and System Science (2008).